

Streamline-Assisted History Matching

Marco R. Thiele, Darryl H. Fenwick, Rod P. Batycky,
Streamsim Technologies, Inc.

ABSTRACT

History matching (HM) is a difficult exercise that generally consumes a large portion of a reservoir engineer's time. When HM is specifically targeted towards improving the underlying petrophysical description of a model—i.e. the spatial permeability and porosity distributions—it quickly becomes a challenging and intractable problem as the number of grid cells and wells increase. All modern history-matching approaches ultimately depend on the forward modeling tool at the engineer's disposal and his or her experience in relating changes in the output response to changes in the input data. A good software environment for the visualization and manipulation of large amounts of data is imperative.

Streamline-based flow simulation (SL) is an effective and complementary technology to more traditional flow modeling approaches such as finite differences (FD). Specifically, SL has some powerful characteristics and data generation capabilities that are valuable in the HM workflow geared towards calibrating the petrophysical description to observed historical production data.

Streamline-based flow simulation is particularly effective in solving large, geologically complex and heterogeneous systems, where fluid flow is dictated by well positions and rates, rock properties (permeability, porosity, and fault distributions), fluid mobility (phase relative permeabilities and viscosities), gravity, and voidage replacement ratios close to one. These are the class of problems more traditional modeling techniques have difficulties with. Modern SL simulation rests on 6 key principles, which are reviewed in this paper.

For the purpose of HM, SL has at least four direct benefits: (a) it is usually a significantly faster simulation tool for displacement-type modeling like water flooding; (b) it captures and quantifies the relationship between injectors and producers in a novel way; (c) it is able to relate the dynamic response at the wells to static properties such as permeability and porosity through the time-of-flight variable along each streamline; and (d) it is able to determine sensitivity coefficients of grid blocks directly from the streamlines.

Although streamline-based HM is still in its infancy, the Judy Creek example shows that with careful implementation it can already be used for problems that would otherwise be prohibitive to do in any other way.

Streamline-Assisted History Matching	1
<i>Abstract</i>	<i>1</i>
<i>The Renewed Interest in Streamlines</i>	<i>3</i>
Flow Visualization	3
Novel Engineering Data: Well Allocation Factors and Well Pore Volumes	4
Computational Efficiency	5
An 80-20 Approach to Reservoir Engineering	6
<i>Historical Context & The Six Key Ideas</i>	<i>7</i>
Key Idea #1: Tracing Streamlines in Three Dimensions Using Time-of-Flight	8
Key Idea #2: Recasting the mass conservation equations in terms of time-of-flight.	8
Key Idea #3: Periodic updating of streamlines.	9
Key Idea #4: Numerical solutions along streamlines	10
Key Idea #5: Gravity.	10
Key Idea #6: Compressible Flow	11
<i>History Matching—A Brief Introduction</i>	<i>13</i>
<i>Streamline-Assisted History Matching</i>	<i>14</i>
Relating production data to static data via TOF	17
The Time Shift	18
Geological Consistency	19
LVM Update	20
PPM	21
<i>Instantaneous Production Profiles (IPP)</i>	<i>22</i>
Constructing the IPP curve(s)	23
<i>Strategies For History Matching</i>	<i>24</i>
One well and one timestep at the time.	24
One well at the time but using information from all time steps.	25
All wells at the same time but over one timestep.	25
All wells and all timesteps at the same time.	25
Final thoughts on HM strategies	26
<i>Example: Judy Creek 'A' Pool Waterflood/HCMF</i>	<i>26</i>
Geological Model Description	26
Production/Injection History	27
Flow Simulation Model Description	28
Field-Level History Match	28

Well-Level History Matching Workflow	29
Geology Updating	30
Timestep Selection and Model Updating	31
Well Selection.	32
History Matching Results	32
Comparison of Static Models.	32
Correction Factors Mapped to Grid.	33
Comparison of Field Level Production Results.	34
Comparison of Well Level Production Results	35
Impact on Solvent Injection Period	38
Conclusions for the Judy Creek Study	38
<i>Acknowledgments</i>	38
<i>References</i>	39

THE RENEWED INTEREST IN STREAMLINES

Although classical, grid-based reservoir flow simulation remains the workhorse for most reservoir engineering (RE) applications, streamline-based (SL) simulation has taken an important place in the toolkit of many practicing engineers as a complimentary modeling tool. A number of papers have clearly shown the applicability of SL simulation to solve RE problems that have traditionally been cumbersome and difficult to model with more conventional techniques (*Mattax and Dalton 1990, Carlson 2003*). But even full physics, finite-difference models are often pre-processed through a SL simulator in the hope of quickly identifying data problems and thereby reducing study times. History matching is one of those workflows where SL's promise to significantly reduce turn-around times. Streamline-assisted history matching is the main subject of this paper.

A number of characteristics are at the center of the renewed interest in SL modeling. These include visualization aspects, novel data such as well allocation factors and well pore volumes, computational efficiency, and finally a general—although slightly misguided—perception that SL simulation is a “simpler” tool to learn and use than a full physics simulator.

Flow Visualization

Certainly one of the attractive features of SL simulation for many engineers is the visual power of streamlines in outlining flow patterns. Streamlines offer an immediate snapshot of the flow field displaying how wells, reservoir geometry, and reservoir heterogeneity interact to dictate where flow is coming from (injectors) and going to (producers). The ability to see the entire flow field at once is powerful, and invariably yields unexpected and surprising flow behavior of the model under consideration. Real fields, even those drilled in regular patterns, rarely show streamlines conforming to the expected distribution of fluids, and it is not unusual to see wells communicating with other wells far outside expected patterns. Good 3D graphics and good coloring schemes for the streamlines further enhance the visualization effect. Coloring by time-of-flight (TOF)¹, or

¹ The time-of-flight (TOF) is natural coordinate along a streamline and represents the time take by a neutral particle to travel a fixed streamline from the beginning to any point along that streamline. The drainage time (DRT) is simply the complement of the TOF and represent the time take for a neutral particle to travel in reverse when starting at the end of a fixed streamlines.

drainage time (DRT), with different cutoffs can vividly capture the growth of the swept areas over time.

The connectivity of the reservoir expressed by the streamlines can also be abstracted into a flux pattern map (FPmap). The FPmap is a schematic display of how injectors and producers are connected and also displays the well allocation factors, data of particular interest to RE's for managing floods of all types (Thiele & Batycky, 2003).

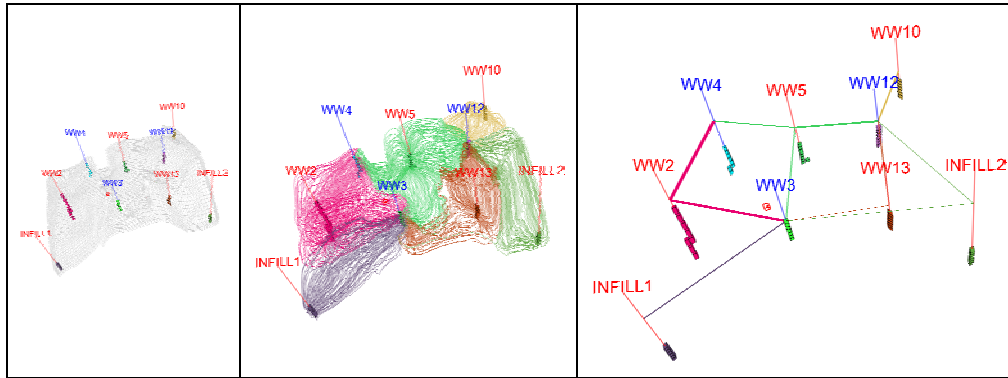


Figure 1: The Flux Pattern Map (right) is a powerful abstraction of information supplied by streamlines (middle), which are traced on the underlying grid (left).

Novel Engineering Data: Well Allocation Factors and Well Pore Volumes

Streamlines go well beyond their visual appeal by producing new engineering data not available from conventional simulation approaches. Producing novel engineering data is potentially the most interesting and valuable contribution of streamlines to the area of reservoir engineering. It is this new data that has had a catalytic effect on history matching and contributed to new developments.

Since streamlines start at a source and end in a sink, it is possible to determine which injectors (or part of an aquifer) are supporting a particular producer, and exactly by how much. A high watercut in a producing well can therefore be traced back to specific injection wells or aquifer influx. Conversely, it is possible to determine just how much volume from a particular injection well is contributing to the producers it is supporting—particularly valuable information when trying to balance patterns. In the past, well allocation data has been generated by “eye balling” rates, using isobaric maps, angle open to flow, and the spatial vicinity of injector/producer pairs as a measure of connectedness—classic reservoir surveillance techniques. With SL simulation, the calculation of which well pairs are connected is automatic and more over accounts for the underlying geological model, a key ingredient to properly predicting reservoir performance (Batycky et al. 2007)

Streamlines also yield drainage volumes associated with producers or irrigation volumes associated with injectors. In other words, SL's make it possible to divide the reservoir into dynamically defined drainage/irrigation zones attached to individual wells. The zones are dynamic because well rates, neighbor activations/shutins, and well completions are continually changing giving rise to SL's that change in time. Properties normally associated with reservoir volumes can now be expressed on a per-well per-time basis, such as oil in place, water in place, pore volume, and even average permeability and porosity.

It is important to underline the fact that flow-based well allocation factors and well pore volumes are data not previously available to the practicing reservoir engineer. The availability of such data has ignited new RE workflows. Streamline-assisted history matching is one such workflow.

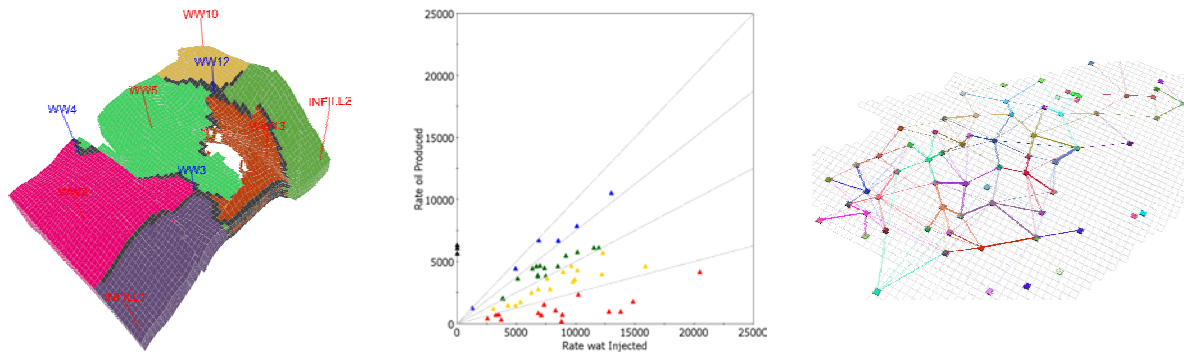


Figure 2: Streamlines produce data not available from more traditional FD approaches such as reservoir volumes associated with individual wells (left), well allocation data between well pairs to calculated injection efficiencies (center), and reservoir connectivity between injector/producer pairs (right). All these combine to a powerful new view of the dynamic behavior of the reservoir.

Computational Efficiency

Computational speed and efficiency are often mentioned as one of the key advantages of SL simulation over more traditional simulation approaches. However, the efficiency comes at a price: simplified flow physics and a non-mass conservative formulation among other things. Certainly for many real fields, the efficiency and speed of SL simulation outweighs the weaknesses associated with the formulation, particular when the uncertainty associated with model parameters is factored in. The opportunity to solve outstanding engineering queries that might otherwise be addressed only with difficulty—if at all—using other approaches is enticing. For example, simulations on multi-million, geocellular models with complex heterogeneity or simulations of equally probable reservoir models to quantify uncertainties in forecast predictions are tailor-made for SL's.

But what makes SL simulation so computationally efficient? SL-based simulation is an IMPES-type formulation and therefore involves only the implicit solution for a single variable, pressure, on the global 3D scale. Tracing of SL's and the solution of the 1D transport problem along each streamline is done sequentially, and thus only one streamline is kept in memory at any given time. Combined with good coding practices, an efficient memory management of grid arrays, and an efficient linear solver such as Algebraic Multigrid (Stüben 2000), it is possible to run finely meshed models on relatively inexpensive computational platforms (PC's) (Samier *et al.*, 2002).

Computational efficiency is additionally achieved because of three main characteristics of SL simulation: (1) the velocity field (i.e. pressure) and associated streamlines only need to be updated infrequently leading to large, global time step sizes; (2) the 1D transport problem along each streamline can be solved efficiently due to a vast amount of literature on numerical schemes in 1D; and (3) the number of streamlines increases near-linearly with the number of active cells of a model. As a result and when combined with an efficient matrix solver, SL simulation exhibits a near-linear scaling of run times with the number of active cells as shown in Figure 3.

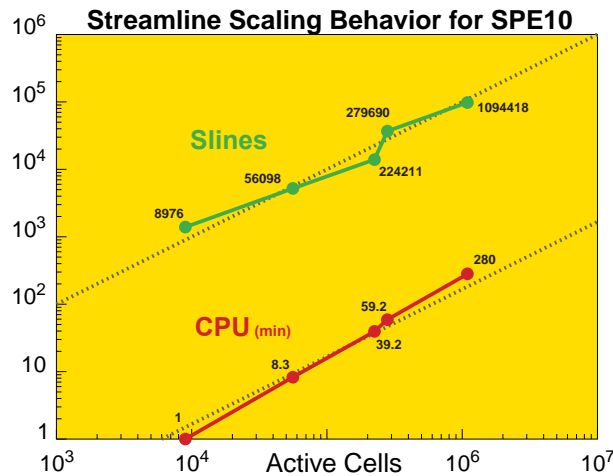


Figure 3: Example of linear scaling of run time and number of streamlines as a function of active cells for the SPE Comparative Solution Project #10 using 3DSL, a commercial streamline simulator, on a PIII 866MHz PC.

The fact that SL's need to be updated only infrequently is a key ingredient for the computational efficiency of SL simulation and deserves special attention. Streamlines change over time due to the spatially changing phase mobilities and, of course, changing well events. However, for many practical problems, grouping well events into yearly or semi-yearly intervals and assuming that the streamlines remain unchanged over that period has proven to yield solutions that have sufficient accuracy for most RE problems. Most importantly and in contrast to more traditional simulation approaches, the size of the global time steps—i.e. the number of SL updates—is insensitive to the mesh size of the model. This has far reaching consequences in RE workflows, since the size of the mesh is linked with the underlying spatial petrophysical description, accuracy of the derived insitu phase distribution, and the reliability of the model for forecasting purposes.

An 80-20 Approach to Reservoir Engineering

There are significant simplifying assumptions used in SL simulation, particularly with regard to flow physics. This is because the technique grew out of an incompressible framework, with the main modeling interest being to gain insight into the field-wide reservoir flow performance, particularly as it pertains to heterogeneity interacting with injected and produced volumes. From the beginning then, the focus for SL's was on roughly capturing field displacement efficiencies, with the explicit understanding that quicker simulations on geologically more detail grids required a trade-off against a more comprehensive description of flow physics. Streamline simulation is a methodology that follows the classic engineering 80-20 rule: finding 80% of the answer in 20% of the time. How effective such an approach can be in the specific case of RE has been presented by *Williams et al. (2004)*, where a top-down methodology—investigating the simplest possible models first and adding details later as required by business decisions—has resulted in an estimated 20% increase in net present value of the projects to which it was applied. In contrast, the all too common bottom-up strategy of using all possible information and the most detailed simulation models from the start risks leaving the engineer overwhelmed and unable to focus on the critical engineering questions at hand.

Today, a bottom-up simulation strategy is no longer sustainable given the model complexities that can be build-in quickly through the use of sophisticated earth modeling software while decision makers face ever-tighter budgetary and time constraints. The ability to rapidly model and produce multiple forecast scenarios is one of the strengths of SL simulation.

HISTORICAL CONTEXT & THE SIX KEY IDEAS

The current popularity of SL simulation should more aptly be termed a resurgence, given that streamlines—as pertaining to modeling subsurface fluid flow and transport—have been in the petroleum literature since Muskat and Wyckoff's 1934 paper and have received repeated attention since then. It is not the authors' intention to give a full review of the technology in this paper. The interested reader is referred to the many papers and dissertations having extensive discussions and reference lists.

The classical approach to determining streamline paths was to use the line source solution and the principle of superposition in two dimensions (2D) under the assumptions of incompressibility, unit mobility ratio, and a homogenous and isotropic reservoir to derive the flux vectors (Caudle 1966)

$$\begin{aligned} v_x &= \frac{1}{2\pi h \phi} \sum_{i=1}^m q_i \frac{(x - x_i)}{(x - x_i)^2 + (y - y_i)^2} \\ v_y &= \frac{1}{2\pi h \phi} \sum_{i=1}^m q_i \frac{(y - y_i)}{(x - x_i)^2 + (y - y_i)^2} \end{aligned} \quad (1.)$$

where m is the number of sources or sinks, including image wells, and q_i is the (constant) volumetric rate of the source (+) or sink (-) located at (x_i, y_i) . The streamlines could then easily be traced from source to sink by using an explicit integration

$$x^{n+1} = x^n + (t^{n+1} - t^n) \times v_x|_{x^n, y^n} \quad ; \quad y^{n+1} = y^n + (t^{n+1} - t^n) \times v_y|_{x^n, y^n} \quad (2.)$$

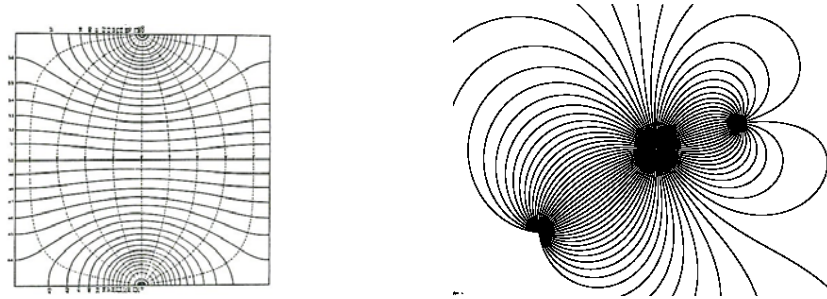


Figure 4: (Left) Streamlines and iso-potential lines for a direct line drive from Muskat and Wyckoff's 1934 paper "A Theoretical Analysis of Water-Flooding Network"; (Right) Streamlines derived using the steady state line source solution and the principle of superposition for an infinite reservoir from B. Caudle's SPE Lecture Notes (1966) on Reservoir Engineering.

Though helpful for basic reservoir engineering analysis, using streamlines derived using the assumptions inherent in the line source solution became too restrictive, particularly when compared to the emerging finite-difference alternative that offered a more general approach to track fluid movement in geologically heterogeneous systems. However since then, streamline based simulation has resurfaced thanks to six key ideas that form the core of the current state-of-the-art of the technology.

Key Idea #1: Tracing Streamlines in Three Dimensions Using Time-of-Flight

One distinguishing feature of current SL simulation is that the streamlines are truly 3D, rather than 2D as in the streamline and streamtube methods of the 70's and 80's. While streamlines are generally depicted from a birds-eye perspective, streamlines now correctly account for the previously missing third (vertical) flow component. Adding the third dimension has been critical to the current success of the technology, capturing cross-flow between layers and flow around geological barriers, and most importantly: gravity. From a practical point of view, the availability of 3D streamlines no longer requires geological models to be transformed into pseudo 2D areal homogenous models. Instead, models can retain a full 3D, geocellular description, and streamlines can appear crossing in a 2D plan view—as in Figure 5—because of the added dimensionality of the problem.

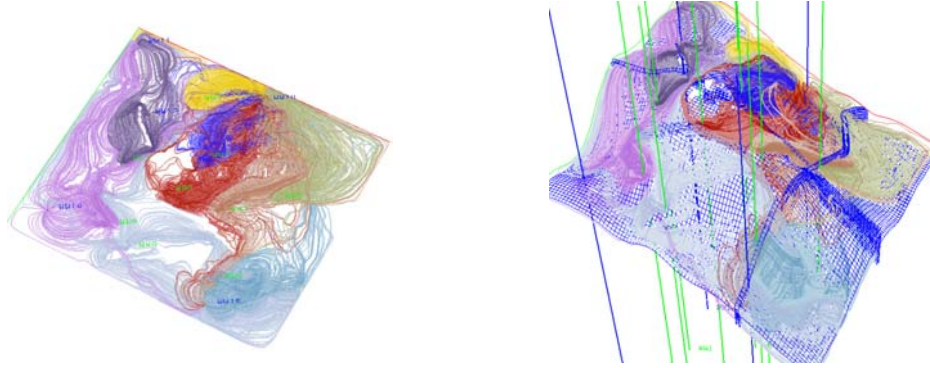


Figure 5: Although SL are generally depicted from a birds-eye perspective and appear 2-dimensional (left), SL's today are truly 3D and properly account for the vertical flow component (right).

The breakthrough work for tracing streamlines efficiently in 3D was that of Pollock (1988). Pollock's method is simple, analytical, and is formulated in terms of a time-of-flight (TOF) coordinate. To apply Pollock's tracing method to any cell, the total flux in and out of each boundary is calculated using Darcy's Law. With the flux known, the algorithm centers on determining the exit point of a streamline and the time to exit given any entry point assuming a piece-wise linear approximation of the velocity field in each coordinate direction. This is consistent with the assumptions inherent in the 7-point stencil used in finite-difference calculation of the pressure field, upon which the velocities are derived from.

Key Idea #2: Recasting the mass conservation equations in terms of time-of-flight.

The understanding that using a TOF-variable along streamlines rather than a volume-variable along streamtubes came through the reformulation of the 3D mass conservation equations in terms of TOF. This was first shown by King et al. (1993) and later expanded on by Datta-Gupta and King (1995). The central assumption in the derivation was that the streamlines did not change over time—an assumption later relaxed as described in the next section. The derivation is simple (Blunt et al., 1996, Batycky et al. 1997, Ingebrigtsen et al. 1999). For incompressible and immiscible flow without gravity, the conservation equation for a phase j can be written as

$$\phi \frac{\partial S_j}{\partial t} + \vec{v}_i \cdot \nabla f_j = 0 \quad (3.)$$

where S_j is the saturation of phase j , $\bar{v}_t = \sum \bar{v}_j$ is the total velocity and f_j is the fractional flow of phase j . Consider the definition of the TOF, which is just the time it takes a particle to travel a given distance along a streamline having a total velocity of magnitude $|\bar{v}_t|$ defined along it. Thus,

$$\tau = \int \frac{\phi}{|\bar{v}_t|} d\xi \quad \rightarrow \quad \frac{\partial \tau}{\partial \xi} = \frac{\phi}{|\bar{v}_t|} \quad \rightarrow \quad |\bar{v}_t| \frac{\partial}{\partial \xi} = \phi \frac{\partial}{\partial \tau} \quad (4.)$$

But notice that along a streamline

$$\bar{v}_t \cdot \nabla = |\bar{v}_t| \frac{\partial}{\partial \xi} \quad (5.)$$

which allows the 3D conservation equation to be re-written as a 1D equation along streamlines in terms of TOF:

$$\frac{\partial S_j}{\partial t} + \frac{\partial f_j}{\partial \tau} = 0 \quad (6.)$$

There are a number of assumptions buried in this derivation: (i) the volumetric flow rate along each streamline is assumed constant; (ii) the streamlines do not change over time (steady state flow); and (iii) the 1D solutions must have the same boundary and initial conditions as the 3D problem. What the derivation does show is that a three-dimensional transport problem can be re-written in terms of a sum of one-dimensional problems along streamlines. While this was known intuitively from the work on streamtubes, the TOF formulation offers a compelling and clear mathematical framework. For the simple case of an incompressible waterflood it is thus possible to write

$$\phi \frac{\partial S_j}{\partial t} + \bar{u}_t \cdot \nabla f_j = 0 = \sum_{streamlines}^{all} \left(\frac{\partial S_j}{\partial t} + \frac{\partial f_j}{\partial \tau} \right) \quad (7.)$$

The most important detail about Eq.(7.) is that the total interstitial velocity (containing permeability and porosity) of the 3D problem has disappeared and is captured in the TOF of each individual streamline. It is this decoupling of a 3D heterogeneous system into a series of 1D homogenous systems in terms of TOF that makes the SL method so attractive.

Key Idea #3: Periodic updating of streamlines.

The fixed streamtube assumption (steady state flow) was probably the single most significant drawback that prevented a wider use of the technology during the 70's and 80's. Martin & Wegner

(1979) and Renard (1990) did consider changing streamline and streamtube geometries with time, but it was not until the mid 90's that the fixed-streamline assumption was relaxed for good (Thiele *et al.* 1996, Batycky *et al.* 1997). At the time, the main interest was to properly account for the rapidly changing mobility field in miscible gas injection problems. The real benefit though was that now changing well conditions—changing flow rates, new wells coming online, and old wells being shut in—and gravity could also be accounted for.

The idea was to treat the problem as a succession of steady-states by considering each updated streamline field valid only for a fixed time interval before updating again. However, this required the ability to solve transport problems with generalized initial conditions along each streamlines (Batycky *et al.* 1997). Streamline geometries could then change at will, guaranteeing that fluids would be transported properly since the initial conditions for the new streamline geometries would be equal to the conditions at the end of the previous timestep.

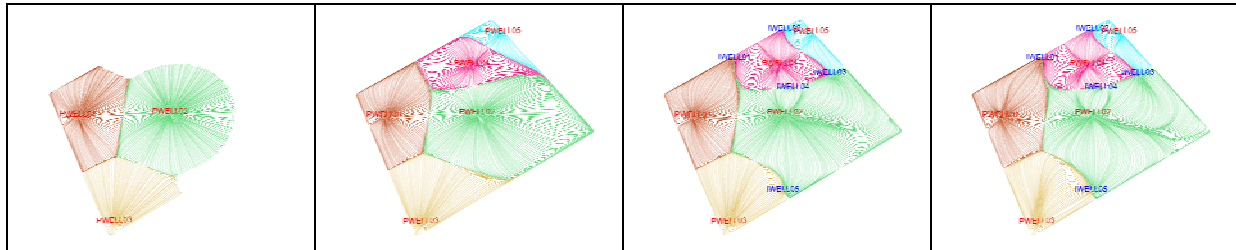


Figure 6: Streamline geometries can change due to changing well conditions—i.e. rate changes, new wells coming online, or wells being shut-in—as well as a changing mobility field. In general, changing wells conditions will have a stronger impact on streamlines geometries than changes in the mobility field alone. From left: streamlines for primary production; 4 producers with drainage zones; 5 additional injectors added to producers; no change in rates or wells

Key Idea #4: Numerical solutions along streamlines

Numerical 1D solutions along streamlines were first introduced by Bommer & Schechter (1979) to solve a Uranium leaching problem. In their work, Bommer & Schechter used fixed streamlines (steady state) and a numerical solution to solve the transport problem along each streamline because there was no analytical solution for the problem they were interested in. Batycky *et al.* (1997) then combined time-varying three-dimensional streamlines with a general, one-dimensional, numerical solution in TOF-space. This merging of ideas was instrumental in allowing streamline-based simulation to be used in real field cases, where streamlines would not only change due to mobility differences but also because of changing well conditions. With every new set of streamlines, the correct initial conditions could be mapped onto the streamlines—the conditions existing at the end of the previous timestep—and moved forward in time numerically. This allowed moving components correctly in 3D despite significant and radical changes in streamline geometries due to changing well conditions. Using 1D numerical solutions also made it possible to consider any 1D solution along streamlines, including complex compositional displacements (Thiele *et al.* 1997) or multi-component contaminant transport in aquifers (Crane and Blunt 2000). More recently, the solution for dual-porosity models has also been solved along streamlines (Di Donato *et al.* 2003, Di Donato & Blunt 2004, Thiele *et al.* 2004).

Key Idea #5: Gravity.

In the presence of gravity, the total velocity vector—to which a streamline is tangent to—is the sum of the phase vectors. However, the phase vectors are typically not aligned. A solution to this

problem was presented by Bratvedt et al. (1996) using the concept of operator splitting, an idea that had found previous application in front tracking (Glimm et al. 1983, Bratvedt et al. 1992) and is a well-known mathematical technique. Operator splitting solves the material balance equations in two steps: first a “convective step” is taken along the streamlines which is then followed by a “gravity” step along gravity lines—lines parallel to the gravity vector \vec{g} . In the gravity step fluids are segregated vertically according to their phase densities only. This is not to be confused with a vertical equilibration problem.

The mathematics is rather simple. The conservation equation for incompressible, immiscible flow can be written as

$$\frac{\partial S_j}{\partial t} + \frac{\partial f_j}{\partial \tau} + \frac{1}{\phi} \frac{\partial G_j(S_j)}{\partial z} = 0; \quad (8.)$$

$$G_j(S_j) = f_j \sum_{i=1}^{n_p} \lambda_i (\rho_i - \rho_j), \quad f_j = \frac{|u_j|}{\sum |u_i|}$$

where G is the density difference driven phase velocities. Operator splitting solves the conservation equation by breaking it up into two, in which the solution of the first part becomes the initial conditions for the next.

$$\frac{\partial S_j}{\partial t} + \frac{\partial f_j}{\partial \tau} = 0; \quad (9.)$$

$$\frac{\partial S_j}{\partial t} + \frac{1}{\phi} \frac{\partial G(S_j)}{\partial z} = 0$$

While the order of the solution is mathematically immaterial, streamline-based simulation solves the convective step first followed by the gravity step, due to the timescale for convective movement versus the timescale for vertical segregation due to density differences.

Key Idea #6: Compressible Flow

All streamtube and streamline work in the past was restricted to the assumption of incompressible flow. The reason, of course, is that incompressible flow introduces simplifying assumptions that are particularly suitable for SL simulation. Two assumptions in particular are worth mentioning:

1. source and sinks correspond to wells (or an aquifer), meaning that all streamlines must start in a source (an injector) and end in a sink (producer); and
2. the flow rate along each streamline (or streamtube) is constant.

This second assumption is particularly important as it implies that transport along a streamline only involves solving for the component wave speeds, and is completely independent of the absolute pressure.

If the flow is compressible then streamlines can start or end in any gridblocks that act as a source or sink, even if the block has no well. For example, in expansion type problems, any gridblock that

sees its volume increase with decreasing pressure is a source and thus a potential starting point for a streamline.

Figure 7 shows streamlines under primary depletion. Streamlines now start in the far field and end in producers that act as sinks, yet there are no ‘real’ sources (injection wells) in the traditional sense. Instead, the sources are all along each streamline, since every gridblock a streamline passes through now acts as a source due the fluid expansion.

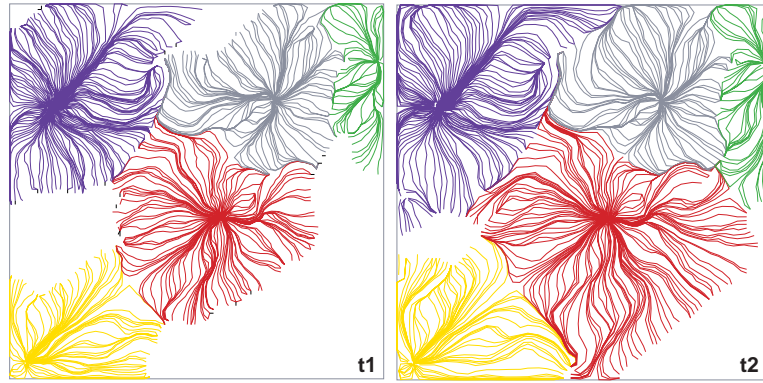


Figure 7: Streamlines shown at two different times during primary depletion. In compressible flow, gridblocks act as sources even though there are no injection wells. A streamline will start in the far field and end in a producer collecting volumes from each gridblock it crosses.

Tracing streamlines in compressible flow remains the same as for incompressible flow, since Pollock’s tracing algorithm is valid regardless of how the flow velocities are determined, so long as the linear independence in each coordinate direction is maintained. The TOF automatically reflects the effects of compressibility, as the velocity field is determined from a compressible formulation in the first place.

A significant extension however is required to account for the coupling between saturations/compositions and pressure that now exists along the SL’s, and that will change along a SL. There is also the additional complication that the flow rate is no longer constant along the streamline. One possible solution has been published by Ingebrigtsen et al (1999) and more recently by (Cheng et al. 2005). An un-published approach has been used in a commercially available code (3DSL 2007) since 1997 and used for modeling compressible immiscible and miscible three-phase systems.

The previous six key ideas are central to the current state of SL simulation. Many mathematical details have been left out in the interest of time and clarity, but the curious reader will find many of the publications referenced to be excellent sources. For a source of how streamline simulation came into being and many details, the reader is referred to Batycky’s PhD Thesis (1997).

HISTORY MATCHING—A BRIEF INTRODUCTION

“History matching” (HM) is generally understood to be the process by which the input data associated with a reservoir simulation model are altered in such a way to match recorded production data (fluid rates, pressures, tracers, temperatures, etc.). History matching is a model calibration exercise. The assumption is that if a model is able to reproduce the past it might be useful to predict the future under various development scenarios and thereby help reduce the risk associated with decisions that are made under the inevitable backdrop of data uncertainty. The purpose of history matching has been succinctly stated by Caers (2005) as *“The purpose of history matching is not just to match history, but rather to produce models that can be used to forecast reservoir performance within some accepted tolerance.”*

The advent of detailed geologic models, the desire to address reservoir uncertainty as it might impact development scenarios, and the availability of lower cost and faster computers have lead to renewed interest in trying to automate the HM process. However, automatic history matching is—and will likely remain—a very challenging task and improbable to ever be fully automated. Production data is an integrated response and a weak constraint for the block-data (petrophysical data associated with the volume support of a single numerical gridblock) associated with a reservoir model. A more descriptive name of what all engineers do today when they calibrate a reservoir model and associated data is assisted history matching (AHM). AHM is a computer-aided history matching workflow that relies on engineering guidance, but which is significantly less cumbersome and more powerful than “traditional” HM by hand. Some of the issues that make HM difficult are:

1. If considered strictly as an inverse problem, AHM is an ill-conditioned mathematical problem that is non-unique and thus has a very large solution set. In other words, reservoir models and simulators have a very large number of parameters, which can be varied. It is difficult for the reservoir engineer to understand which parameters should be modified and in what manner.
2. The physics of most models is non-linear—in many cases strongly non-linear—meaning it is not possible to easily relate changes in the output data to changes in the input data.
3. Extensive sensitivity studies are generally required to gain a good understanding of the reservoir model and how to calibrate it. These are rarely done.
4. Some input parameters are stochastic in nature, particularly data describing the spatial, petrophysical distribution. In such cases, it should be the parameters describing the statistics that should be changed rather than the outcomes. Again, this is rarely done.
5. Production data – particularly old data - is unreliable and often associated with large errors. These are rarely considered in HM.

Beyond the difficulties outlined above, simple questions such as “what to HM” and “when a model is considered HM’ed” don’t have simple answers. However there is consensus that matching at the field level is significantly easier than matching well-by-well responses. A field-level match means capturing the integrated total reservoir volumes injected/produced while calculating an average field pressure behavior that parallels the observed pressure data. It is worth noting that there is no such thing as a historical “average pressure” measurement. Instead, the average field pressure is generally reconstructed from flowing well pressures, well tests, and/or observation wells. This has important implication when making the decision of what a good field pressure match actually is. The inability of obtaining a field match is often a good indication that the starting reservoir model is inconsistent—incorrect pore volume(s), incorrect compartmentalization, improper PVT description, wrong initialization, etc.—and in need of revision. Once an acceptable field match is achieved, the next step is to begin matching regional pressure and saturation distributions and individual well phase rates. This is also known as individual well matching.

Matching individual well behavior is a much more difficult problem in HM, in part because of the large amount of variables (all phase rates and pressures of all the wells for all times) but mainly because locally fixing the behavior for one well might break a previously matched neighboring well. History matching at the individual well level can be viewed as an optimization problem, which has led many researchers to frame it within traditional optimization frameworks (gradient methods, global search methods, etc). This works well when the number of variables one changes remains small, as might be the case when HM'ing using relative permeability curves, fluid viscosities, or aquifer strength. It does not work well when the number of variables is large, as is the case when modifying petrophysical properties associated with the reservoir grid. In such cases, the potential search space is so large that finding the global minimum of the objective function is impossible in practice despite the fact that a number of methodologies exist to find local minima—gradient methods, global search methods, and more recently Ensemble Kalman filters. While these methods can in some circumstances give acceptable solutions for short term forecasts, the complex spatial correlations typical of petrophysical properties are difficult to model correctly within traditional optimization frameworks. Very few researchers address this problem. One approach is to use streamlines. Streamline-assisted history matching allows for the consistent modification of the reservoir model while retaining the complex spatial correlations among properties. When combined with the speed and efficiency of the computational SL engine, the hope is that turn around times for creating calibrated models that can be used for forecasting is reduced.

STREAMLINE-ASSISTED HISTORY MATCHING

Having an efficient computational method like SL simulation to quickly generate reservoir responses is an advantage even in the context of more traditional HM techniques. Faster forward simulations allows the engineer to rapidly evaluate many reservoir models while using a finer computational mesh—i.e. a larger number of gridblocks between wells—which is known to reduce the numerical artifacts that can mask true physical effects.

However, SL-assisted history matching (SLAHM) differentiates itself from other AHM techniques in that it makes use of SL-specific data, such as the SL trajectories, the TOF variable associated with each SL's, and the dynamic well drainage regions. There have been three main approaches to using SL's for history matching in the past:

1. Defining average reservoir regions associated with wells and then changing permeability directly (applying multipliers) in these regions to match production response (*Emanuel and Milliken 1997,1998*);
2. Derivation of analytical sensitivity coefficients which are then used to set-up an inverse problem using traditional optimization techniques (*Wen et al. 1998, Vasco et al. 1999*);
3. Modify grid properties traversed by streamlines to reduce/increase breakthrough times along these streamlines (*Wang and Kovscek 2000; Caers et al. 2002, Agarwal and Blunt, 2001,2004*).

All three methods have shown to be useful in a variety of settings under different operating conditions. The AHM approach of Emanuel and Milliken (*1997,1998*) has been applied on a number of real fields. By defining average regions (areas of influence) that are associated with production wells, the approach used the Dykstra-Parsons coefficient to modify the existing permeability distribution. The method does not rely on any formal convergence criteria, and instead requires the engineer to use judgment and experience to decide by how much to modify the underlying geological model parameters. In the usual manner, the updated model is re-run and checked against field performance. The process is continued until an acceptable match is achieved.

The ability to derive analytical sensitivity coefficient from streamlines is a particularly powerful characteristic of SL's and has been used by several authors for HM (Wen *et al.* 1998, Vasco *et al.* 1999, Wu and Datta-Gupta 2002). Once the sensitivity coefficients are known, the method is framed as a classical optimization problem and is shown to lead to a good HM if the initial model is not too far from “the solution”. However, the inherent assumption when deriving the sensitivity coefficients—that the streamlines do not shift significantly because of small perturbations in reservoir properties (Wu and Datta-Gupta 2002)—and that sensitivity coefficients are only defined for continuous variables (permeability/porosity) restrict the application of the method. For example, the location of a channel facies would be very difficult to modify using this approach.

Wang and Kovscek (2000) and Agarwal and Blunt (2001, 2004) have presented direct modification of gridblock properties associated with individual streamlines by using the TOF information to either “speed-up” or “slow-down” the water traveling along individual SL's. This approach can induce large changes in the petrophysical properties and therefore also large changes in the response at the wells. However, the final geological model will not honor the prior geological information and often will exhibit streamline-like features. What can happen when local changes are mapped directly onto the underlying grid can be seen in the rather extreme example shown in Figure 8. Changing permeability directly along the streamline paths results in an unrealistic permeability distribution (Figure 8-right) that has little resemblance with the original geology, although the history match is perfectly acceptable (not shown here).

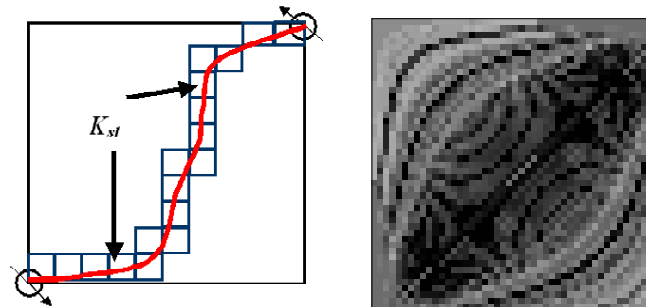
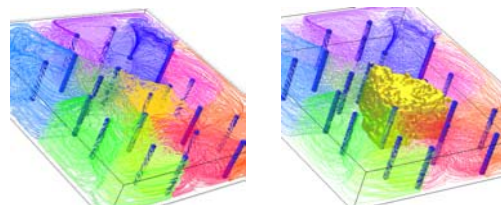


Figure 8: Mapping permeability changes from streamlines directly to the underlying grid causes inconsistent images of the geological model.

An extension of the work of Wang and Kovscek (2000) and Agarwal and Blunt (2001,2004) has recently emerged in the context of geostatistical methods for history matching under geological control (Caers *et al.* 2002, Caers 2003, Le Ravalec-Dupin and Fenwick 2002, Gross *et al.* 2004, Caers 2005). The main idea is to use the ability of SL's to divide the reservoir into zones associated with wells, much in the same spirit as suggested by Emanuel and Milliken (1997,1998).



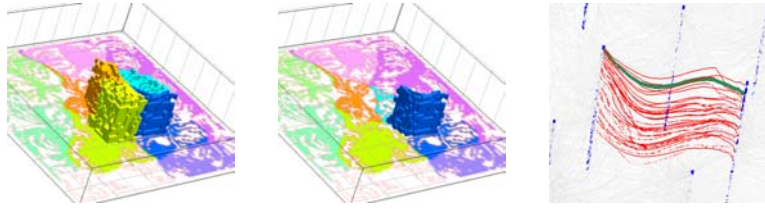


Figure 9: At any particular time (set of streamlines), it is possible to associate volumes of the reservoir (grid blocks) with individual wells. There are three scales of interest SL's are able to define: (a) the volume associated with a drainage/irrigation zone of a well; (b) the volume associated with a well-pair; and (c) volume associated with an individual streamline (courtesy H.Gross).

Perturbations of petrophysical properties can then be applied at three different scales (Figure 9) as driven by mismatches at the production wells, however with the constraint that the prior geological continuity model be honored at all times. This means that the perturbations are not applied directly to the underlying grid, but rather to the parameterization of the geological continuity model. In other words, the perturbations are used as soft conditioning data when creating a new realization using the prior geological scenario. The basic idea is illustrated in Figure 10. Streamlines are used to identify regions (grid blocks) that need to be changed (left). This creates a multiplier/indicator map (center) that can be used as constraining data when updating the petrophysical realization.

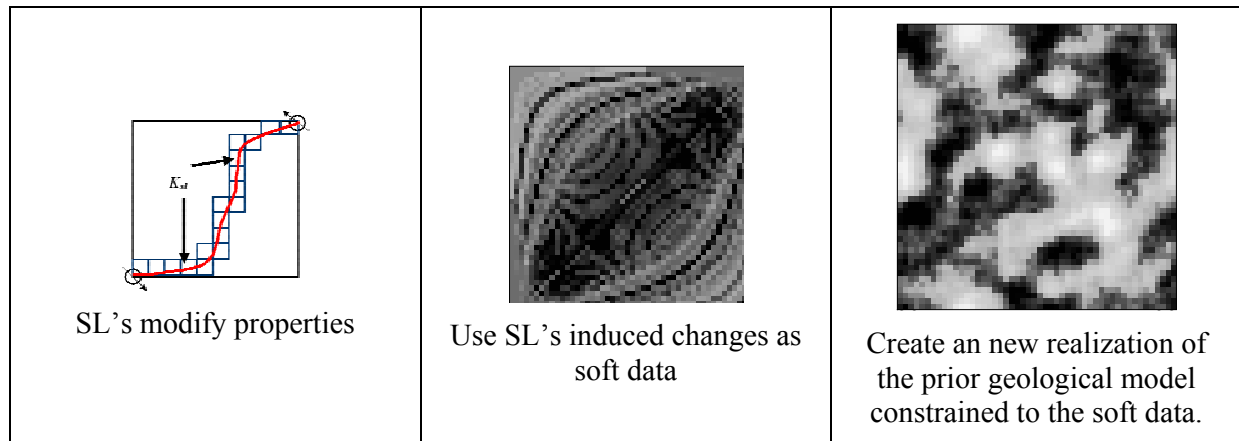


Figure 10: Mapping permeability changes from the streamlines (left) directly to the underlying grid creates the soft data (middle) that is used to constrain the final geologically consistent image (right) (courtesy of J.Caers).

There are two significant implications that follow from this approach:

1. At any iteration in the HM process, the geological model will be consistent and therefore geologically realistic. Geological consistency greatly improves the reliability of the model for forecasting purposes, since in general there are multiple data conditioning sources and a geologically consistent realization simply means that all data (hard and soft) is being accounted for.
2. If the prior geological scenario described through the parameterization is wrong, there is nothing in the HM process that will correct this. In other words, the HM approach will not be able to generate an alternate geological scenario—it can only hope to find an acceptable geological realization from the set of realization that can be built for a particular scenario. If the solution is outside of this set, the methodology will never find it.

Streamlines have two distinct characteristics for AHM:

1. since the streamlines connected to a producer are responsible for the simulated production response (through the numerical solution of a transport problem along each streamline—see key idea #4), and since in turn it is known which gridblocks the SL's traverse on their way to the production well, it is possible to relate the mismatch between simulation and historical production data back to specific locations and petrophysical properties along the path traversed by the SL's; and
2. streamlines are able to quantify by how much to change the petrophysical properties so as to increase/decrease water production.

Relating production data to static data via TOF

The time-of-flight is the time it takes a neutral particle to travel along a streamline. Using the definition of TOF, it is simple to show that the TOF along a streamline is proportional to permeability and inversely proportional to porosity:

$$\tau = \int \frac{\phi}{|\vec{v}_t|} d\xi = - \int \frac{\phi}{k\lambda_t |\nabla P|} d\xi \rightarrow \tau \propto \frac{\phi}{k}. \quad (10.)$$

The porosity enters in Eq.(10.) because fluids travel at the interstitial velocity through porous media. Consider now a generic mismatch between historical and simulated water production for a particular producer as shown in Figure 11.

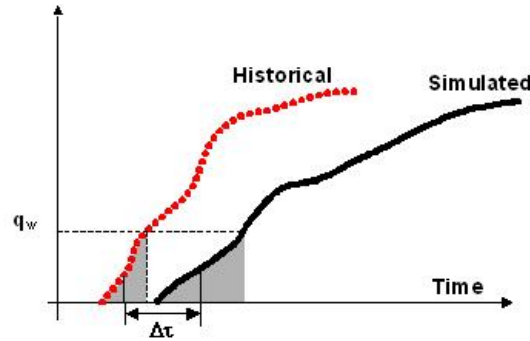


Figure 11: The time-mismatch between historical production data and simulated data defines a TOF-correction that can be applied to individual streamlines as per Eq.(11.).

For now, assume the following: (a) water moves along each streamline in a piston-like fashion and (b) assume the streamlines are fixed in the simulation model for the time period over which the mismatch is measured. The desire is to shift (to the left) the simulation curve by an amount Δt such that the mismatch between historical and simulated water production is minimized. In other words, streamlines that are breaking through too late compared to historical require a reduction in their TOF, which is equivalent to making water travel faster. Since we are assuming that the streamlines are fixed (fixed pressure drop) and that the flow is piston-like (constant total mobility), increasing/decreasing the TOF becomes a function of the average porosity/permeability ratio along a SL only. The question then is: what should the average porosity/permeability ratio be so as to shift the production curve (to the left, in this case)? Since we have inherently assumed the flow to be linear, we can write for each SL that:

$$\frac{\tau^{new}}{\tau^{old}} = \frac{\left\langle \frac{\phi}{k} \right\rangle^{new}}{\left\langle \frac{\phi}{k} \right\rangle^{old}} \rightarrow \left\langle \frac{\phi}{k} \right\rangle^{new} = \frac{\tau^{old} + \Delta\tau}{\tau^{old}} \left\langle \frac{\phi}{k} \right\rangle^{old} \quad (11.)$$

where the average porosity/permeability ratio is calculated as a resistance in series expression along a streamline (see Figure 8) as follows

$$\left\langle \frac{\phi}{k} \right\rangle = \frac{1}{\tau} \sum \Delta\tau_i \left(\frac{\phi}{k} \right)_i \quad (12.)$$

where the $\Delta\tau_i$ is the TOF associated with the SL segment traversing a gridblock with ratio $(\phi/k)_i$.

Notice a few important things about Eq.(11.). There is an inherent assumption on the sign of Δt . If the simulation curve is slower than the historical curve—i.e. the simulation curve is to the right of the historical production curve—then Δt is assumed positive. On the other hand, if the simulation curve is to the left of the historical production curve, then Δt would be assumed negative. It is easy to see why. To speed breakthrough, we have to either increase permeability and/or decrease porosity. In other words, the ratio (ϕ/k) has to go down. Conversely, if we want to slow things down, then the ratio (ϕ/k) has to increase. This implies a sign on Δt .

To summarize, a key benefit of SL simulation is that not only does it identify whether to increase or decrease (ϕ/k) but it also is able to quantify by how much and where to change (ϕ/k) to improve a match.

The Time Shift

Figure 11 and Eq.'s (11. and (12.) are particularly attractive because the time-shift Δt is easily related to the natural TOF-variable that is known along the SL's. However, there are a few subtleties that revolve around Δt that need to be addressed.

The time-shift is determined by fixing a value on the ordinate (say water production rate), determining the intersection point with the historical and simulated production curves, and then reading the time-shift from the abscissa. In other words, there are multiple time-shifts as one compares the historical and simulated curves at various values along the ordinate. Since each time-value of the simulated curve is associated with a SL-map, it is possible to associate the time-shift Δt with a particular SL-map. However, this is strictly true if and only if there are no new well events between the two times used to calculate the time shift. Figure 12 illustrates this idea.

The time t_1 is the time associated with the historical observed water production q_w . For the same q_w , the simulated curve gives a time t_2 , which in turn results in a time-shift of $\Delta t = t_1 - t_2$. Since the time shift is used to modify the petrophysical properties along the streamlines, the assumption is that both times have essentially the same streamline geometries (well connections), only that in the simulated case, fluids move too slowly (or quickly) along the same SL's. Modifying the petrophysical properties as per Eq.(11.) would then lead to a proper time shift in the simulated curve and thus an improved history match.

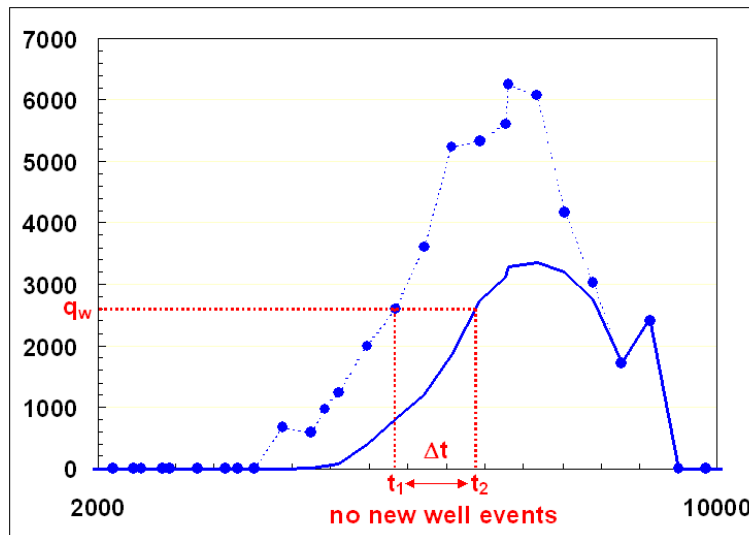


Figure 12: The time-shift $\Delta t = t_1 - t_2$ is strictly valid if and only if approximately constant streamline geometries (no new well events) between the time t_1 (the time associated with the historical value of q_w) and t_2 (the time associated with the simulated value of q_w).

However, consider the case where there is a significant difference between t_1 and t_2 (new wells coming online or wells being shut-in or wells experiencing significant well rate changes or all of the above). Applying the time-shift to the SL's of the simulated curve at t_2 would be incorrect, since the SL geometries at time t_1 and t_2 are likely to be very different. And consider the extreme case, where one of the two curves is missing altogether. For example, there might be a historical water profile but no simulated water profile or vice versa. In which case there is no definition of the time-shift at all. We will come back to this point by introducing the instantaneous production profiles (IPP's).

It is also possible to define an average time-shift over the entire simulation period. This would be a time-shift that minimizes the difference between the simulated and historical profile, by considering the L1 or L2-norm. Such an approach has been taken by Wu and Datta-Gupta (2002). However, as in the previously described case, if streamline geometries are not approximately constant, or if one of the curves is missing then even an average time-shift will not be defined.

Geological Consistency

The most powerful aspect of SLAHM is the data integration aspect and geological consistency with the prior model. In principle, the data integration workflow could also be used when using standard box-type multipliers. However, SL's have the significant advantage of being able to pinpoint much more accurately where to modify the geological model and by how much.

The basic workflow for achieving geological consistency is outlined in Figure 13. Previous conditioning data (core data, seismic, well-test, etc) combined with a prior geological model are used to create a realization of the reservoir, i.e. a spatial distribution of all petrophysical properties required by a simulation model. At this point, historical and simulated production curves are compared. If the HM is deemed acceptable using some sort of criteria—for example, 80% of the wells have an error less than 10% as measured by cumulative water production—then the loop is stopped. Otherwise, each well is used to determine a time-shift which is then translated into a correction factor (a multiplier) and mapped using the streamline paths onto the grid. The

correction-factor map is then used as soft conditioning data by either updating the local varying mean (LVM) or the probability perturbation method (PPM) and then combined with previous condition data and the prior model to generate a new realization of the reservoir. The loop is then repeated until a convergence criterion is reached.

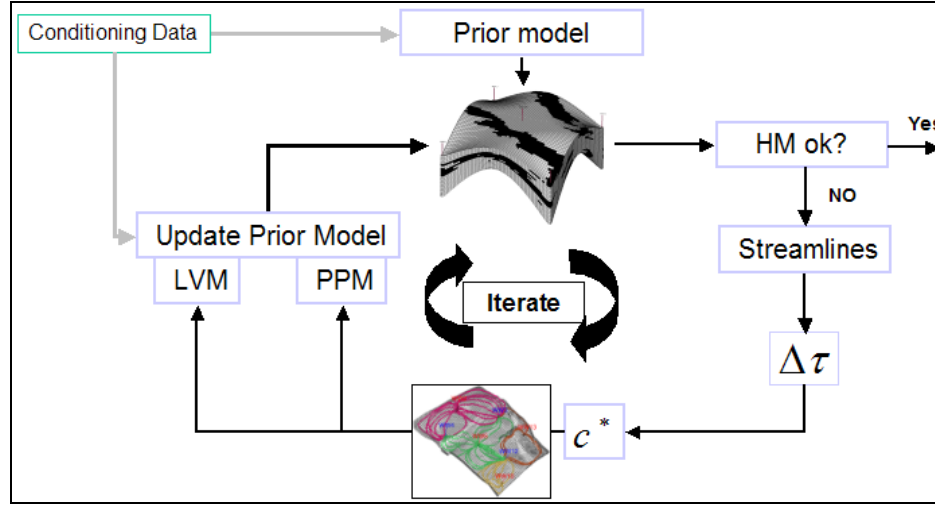


Figure 13: SLAHM data-integration workflow for achieving geological consistency.

LVM Update

Although the SLAHM approach has geological consistency as one of its cornerstones, it is not the intent of the authors to give a detailed description of the geostatistical algorithms used to achieve this goal. Only a brief overview is given here to allow the reader to grasp the general concept. For an excellent overview on geostatistics, the reader is referred to Caer's (2006) primer, which also contains references to other resources.

The local varying mean (LVM) update approach is closely linked with the stochastic simulation of continuous variables such as permeability or porosity. In direct sequential simulation (DSSIM), for example, the unknown property z at a location \mathbf{u} , is estimated by a linear combination of neighboring properties z at locations \mathbf{u}_α and the mean m at location \mathbf{u} . The expression is written as

$$z^*(\mathbf{u}) = \sum_{\alpha=1}^{n_1} \lambda_\alpha z(\mathbf{u}_\alpha) + \left(1 - \sum_{\alpha=1}^{n_1} \lambda_\alpha\right) m(\mathbf{u}) \quad (13.)$$

The kriging weights λ_α in Eq. 13. are determined by solving simultaneously a set of n_1 equations using the covariance function for the property z (which may be permeability, porosity, NTG, etc).

$$\sum_{\beta=1}^{n_1} \lambda_\beta^{(1)} c(\mathbf{u}_\beta - \mathbf{u}_\alpha) = c(\mathbf{u} - \mathbf{u}_\alpha) \quad \alpha = 1, \dots, n_1 \dots\dots \quad (14.)$$

The weights λ_α thus account for the spatial correlation of the variable z in the reservoir. The (local) mean value m at location \mathbf{u} is assumed to be known (the LVM). It is this LVM that the approach modifies. In summary, when using LVM updating, the attempt is to vary the mean up or down for each grid block by a factor c^* , which is determined from the time-shift in the simulated production curve as compared to historical data. The new average permeability at location \mathbf{u} is thus given by

$$\langle k(\mathbf{u}) \rangle^{new} = \bar{c} * \langle k(\mathbf{u}) \rangle^{old},$$

which is then used as the new mean $m(\mathbf{u})$ in **Eq. 13**. The permeability field is therefore reconstructed by running DSSIM with the updated LVM for each grid block. Note that increasing the LVM of permeability for a grid block does not guarantee that the resulting permeability value at that location will actually increase by a factor of \bar{c} . Rather, increasing the LVM is really increasing the probability that the permeability at that location is higher than it was before. However, if one were to average the permeability at that location across many realization, the average would in fact be the increased LVM.

If the permeability differs in the horizontal and vertical directions, then the LVM updates are performed in an identical manner in each direction. Note also that we are neglecting the effect of porosity in the expression for the effective resistance of a streamline bundle (**Eq. 5**) and instead are trying to increase/decrease the phase velocities along the streamlines by only modifying permeability. This is equivalent to saying that

$$\left\langle \frac{k}{\phi}(\mathbf{u}) \right\rangle^{new} = \bar{c} * \left\langle \frac{k}{\phi}(\mathbf{u}) \right\rangle^{old} \rightarrow \frac{\langle k(\mathbf{u}) \rangle^{new}}{\langle \phi(\mathbf{u}) \rangle} = \bar{c} * \frac{\langle k(\mathbf{u}) \rangle^{old}}{\langle \phi(\mathbf{u}) \rangle} \rightarrow \langle k(\mathbf{u}) \rangle^{new} = \bar{c} * \langle k(\mathbf{u}) \rangle^{old},$$

which is not strictly correct. However, the hope is to push the HM in the right direction. The workflow is repeated until the objective function no longer decreases or bounces around, at which point the probability perturbation method (PPM) is applied.

PPM

After the large-scale permeability trends have been captured by using the LVM approach, PPM allows to vary the fine-scale variability of the permeability field without changing the large-scale trends. Previous papers have principally described the PPM in the context of modifying facies values (*Hoffman & Caers 2005*), however here it is used to modify a continuous value (i.e. permeability). For a detailed description on the implementation of the PPM for continuous variables using DSSIM, see Fenwick *et al.* (2005).

Effective use of the PPM relies on the ability to divide the reservoir into drainage regions for each producer. Streamline trajectories are ideal for identifying drainage regions. However, PPM requires these regions to be fixed, whereas the actual drainage regions for each producer change in time, as the production rates change and/or new wells are added to the reservoir. Consider, for example, a well that is shut-in for a period. There is no drainage region associated with the well until it comes on-line, and as the well rate changes in time so too will the region. Note that even in the case where all the well rates are constant in time, streamlines and therefore the drainage regions may still change due to the nonlinear nature of the flow. However, for traditional waterfloods in heterogeneous reservoirs this effect is small when compared to impact of well rates and/or locations. For more strongly nonlinear displacements, such as miscible gas injection or CO₂ flooding, the changes in streamline geometries solely due to spatial variability of fluid properties may be more significant.

What the correct “average” fixed drainage volume to use for a well—or indeed a group of wells—for the PPM to be successful is an open area of research. A number of avenues are being pursued: from a simple averaging with a cutoff to using sensitivity coefficients as a mask. Simple averaging retains any grid block that is part of $x\%$ or more of the drainage regions. In other words, if a particular grid block is part of 75% or more of all the drainage regions associate with well P1 over

time, then it will be part of the average region to use with PPM when trying to modify the local variability. This approach is likely to favor inclusion of grid blocks that are close to the well itself, whereas grid blocks further away might be excluded. Using sensitivity coefficients, on the other hand, tries to identify blocks that have a large impact on the well response regardless of the number of regions and time and assembles an average region that way. A hybrid of the two is also a possibility. Hoffman and Caers (2005) have also presented an attractive approach on how to define PPM regions using streamlines while minimizing the problem associated with grid blocks potentially belonging to different regions.

Once the drainage regions have been fixed, each fixed region i is assigned a perturbation parameter, denoted r_{Di} . By treating the response at well i as being exclusively dependent on the properties in its region, it is possible to perform a series of 1-D optimizations, with one optimization parameter (r_{Di}) per well. The 1-D optimizations are controlled by the individual objective functions at each well and can take any of the standard forms that express the mismatch between simulated and historical data at the well. What the optimization parameter (r_{Di}) controls is how the small-scale variability within the fixed region is reassigned. An $r_{Di}=0$ means that permeability values within the region i remains the same (no re-arrangement), while an $r_{Di}=1$ means that an entirely new realization is generated for that region alone. Any value in-between ($0 < r_{Di} < 1$) is a realization that is somewhere between the current distribution of permeability and an entirely new (but equiprobable) one for that region. In other words, the r_{Di} value serves as an interpolator between two geostastical images, but the key is that the interpolation is in the probabilities of the images, not the images themselves. For each optimization step (or changes in r_{Di}), there is a flow simulation. Once the optimization has converged—i.e. there is no noticeable change in the objective function, a new geostatistical image ($r_{Di}=1$) is created, new regions may be reconstructed, and the process can be repeated.

Note that although the perturbations are performed regionally (the r_{Di} changes the probability attached of each grid block), the geostatistical and flow simulations are performed globally. This ensures that that geological consistency is maintained across regions and no artifacts are introduced across region boundaries. For example, for channel systems, modification of the location of a channel in one region will influence the location of a channel in an adjacent region. In addition, the channel will always be connected across region boundaries.

INSTANTANEOUS PRODUCTION PROFILES (IPP)

The most important component of the SLAHM approach is relating a time-shift between simulated and historical production profiles to the grid blocks—and the static petrophysical properties associated with them—via the SL's. However, as the following discussion outlines, choosing the “correct” streamline map, and streamline bundles within each map, to associate a time-shift and correction factors with is not trivial.

Consider the production curves shown in Figure 11. The same water production happens earlier in the historical observed data than in the simulated curve. For ease of discussion, we will call the times associated with the water production rate Q_w , t_h and t_s , where “h” and “s” stand for historical and simulated respectively. In this particular case $t_h < t_s$ and we find that we need a time-shift of $\Delta\tau=(t_s-t_h)$ which in turn we can associate with an increase in the average permeability/porosity ratio along the streamlines as discussed previously. However, a number of well events might have occurred in the time period between t_h and t_s , so that the streamlines at t_s are not representative of the flow at time t_h . In other words, we cannot apply the correction to the streamlines at t_s to “push” the production curve towards t_h . For real fields, this is the rule rather than the exception.

One solution to this problem is by introducing instantaneous production profiles (IPP's). The IPP curve is constructed by fixing the streamlines at time t_h and then moving the transport solution

forward in time. In other words, the IPP curve is our window into the future well's production for the current set of streamlines, only. The idea is straightforward. The SL's that exist in the simulation model at time t_h reflect the boundary (well) conditions associated with the production data at that time. If we now assume that the SL's remain fixed for all times from that moment on, we can construct a new simulation curve—which as mentioned previously may be very different from the simulation curve that we have considered so far. We call this new simulation curve the IPP curve, and use this curve, rather than the actual simulated production profile to estimate the time-shift.

Constructing the IPP curve(s)

For every streamline map—or alternatively for every time t_h —there exists an IPP curve that can be used to determine the proper time-shift and associated correction factors to use for updating the underlying geomodel. But how expensive is it to construct the IPP curves? The rigorous way, of course, is to run the streamline simulator forward in time maintaining the well constraints existing at time t_h (blue lines in Figure 14). In other words, the model is run up to time t_h using the historical data, and which point the simulation is run forward by using the well rates exiting at time t_h until the water production of the IPP curve is equal to the water production of the historical curve. This guarantees that the same streamlines as those existing at time t_h in the historical model are used to evaluate the time-shift. If t_h occurs early in the simulation, then constructing the IPP curves in this manner might not be that expensive. Note that one simulation gives rise to an IPP curve for all active wells. For wells that breakthrough early, which are often of particular interest, constructing the IPP curves might be reasonable in terms of computational costs. On the other hand, for wells that breakthrough late, the cost to construct the IPP curves will be significantly higher.

It is possible, however, to use a much cheaper proxy for the IPP curves when the simulation curve is later in time w.r.t. the historical curve. For this particular case, one can walk “back” along the streamlines and estimate what the water production would like by simply assuming that the water will move along the fixed streamlines at a unit speed (red lines in Figure 14). This proxy only works for wells where the simulated water production is “later”—i.e. to the right of the historically observed data and can help speed-up the history matching loop significantly, particularly for large models. To some extent, however, the cost is offset by the need to remember all the streamlines with associated properties. For large models, this can be expensive.

For the opposite case—where the simulation curve is “earlier” than the historically observed data—there is no simple proxy. All one can do is slow down the water among all the streamlines that have water on them.

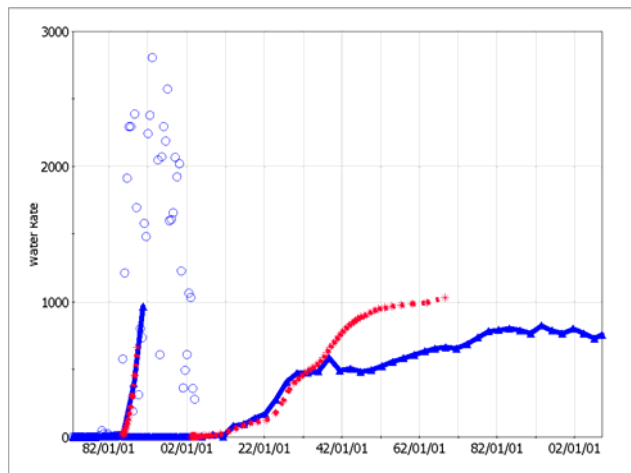


Figure 14: IPP curves at two different times t_h and associated historical production data (open circles). Blue lines are IPP curves constructed by running the streamline simulator forward in time with well rates fixed at the values of t_h . Red line are IPP curves constructed by simply walking backwards along the streamlines.

STRATEGIES FOR HISTORY MATCHING

Among experienced practitioner of history matching workflows, it is a well-known fact that the strategy used to pursue a well-by-well history match can make a significant impact on the turn-around time required to obtain an acceptable match. The key is to pick wells (or group of wells) that are reasonably independent of each other and match them sequentially. Matching the “heavy hitters” first—wells with large rates and a significant mismatch—before proceeding to other wells seems to be a generally accepted approach. The hope is that a previously hard-fought match is not undone as progressively more wells are matched, although this will invariably happen. Such a sequential strategy has the advantage of keeping the problem tractable while ensuring that the largest mismatches are corrected first. However, there is no clear strategy that will work for all cases all the time. Success or failure of any particular approach is closely linked with the initial model, the root of the history mismatch in the first place, and ultimately with experience of the modeler.

Strategy plays an important role in SLAHM as well. In addition to the basic idea of progressively going through a list of well as mentioned previously, there is choice whether to HM using all time steps at the same time or whether to progressively HM sequentially in time. Table 1 summarizes the possible approaches. Note that in reality one can use a subset of timesteps as well as a subset of wells, so that Table 1 is really just illustrating the four limiting cases. These are described next.

		Timesteps	
		One timestep	All timesteps
Wells	One well	1 well and 1 TS at the time.	1 well at the time but using information from all TS's.
	All wells	All wells at the same time but only over 1 TS.	All wells and all TS's at the same time

Table 1: Possible history matching strategies using SLAHM.

One well and one timestep at the time.

This is probably the most conservative strategy, but also the most linear and easily understood. Given a starting reservoir model that needs to be history matched, the user ranks the wells that must be history matched. The order in which the wells are ranked can be determined from a simple L1-norm type metric or a more subjective metric of the engineer's liking. Once the well order is established, HM is initiated one time step at the time. In other words, if well P1 is picked as being the first well to match, P2 the second, and so on, then the first step would be to match P1 over the range of time steps it is active. The obvious first choice might to pick the breakthrough time— t_{br} —of well P1, determine the c^* 's to use and apply it to the drainage region at that particular time as outlined by the streamlines, modify the underlying geomodel, and re-run the simulation. If the breakthrough time is already matched reasonably well, then one simply finds the first time at which

there is a substantial mismatch. Since the well made it at the top of the rank of mismatched wells, there must be times where the mismatch is significant. Note that there is no need to run the simulation all the way to the end of history. All that is needed is to run the simulation until just beyond the time that was picked for HM. Once an acceptable HM at the time of interest is achieved, the next time is picked. There is no guarantee, of course, that a match obtained at a previous step is not destroyed by a later correction. The hope, of course, is exactly the opposite: that early matching will actually improve later time behavior so that as one marches through time less and less work is required. There is also hope that matching this one well will also impact the history match of other wells in a positive fashion. If the opposite happens, however, then it might be a good indication that there is something seriously astray with the initial starting model. In other words, as one progresses through time and previous matches consistently become worse, then it might be an indication that the geoset itself might not be appropriate or that the mismatch is really caused by other model parameter(s). The most important characteristic of the one-well one-TS strategy is that the region to modify is well defined, since there is only one set of streamlines used to outline the area to modify on the grid.

One well at the time but using information from all time steps.

Instead of moving forward one timestep at the time as in previously discussed strategy, the engineer might hope to accelerate the convergence of the HM by using all the streamlines associated with the well over time. This invariably leads to having to define an average region of influence for the well and applying an average c^* to this region. This can be an attractive strategy, particularly if the drainage of a region does not change too dramatically over time. On the other hand, if the region does change significantly because of changing well rates or new wells coming online then such averaging can become a problem. For example, for one particular timestep the $c^* > 1$ meaning that flow needs to be accelerated, but for a later timestep one might find that $c^* < 1$ creating a conflict. The one-well all-timestep strategy clearly has the benefit of more information to guide the HM, but this information might also be in conflict thus requiring some intelligent averaging scheme.

All wells at the same time but over one timestep.

This strategy is particularly attractive, because there are no conflicts in c^* nor in drainage regions associated with the producing wells, yet changes are made to all the wells at the same time. A significant change in the geoset can be expected using this strategy, and it might in fact be the most effective approach to get things going initially. A related strategy, of course, is to select a subset of wells over one timestep. Either way, the advantage of this strategy is that no conflicts in c^* are introduced, nor are there any overlapping drainage regions to worry about (since only the current set of streamlines is being used). This is the strategy used in the Judy Creek example that is presented next (Batycky *et al* 2007).

All wells and all timesteps at the same time.

This strategy is the cheapest in terms of runs, but also the one prone to the largest amount of conflicting information. Depending on the initial state of the match, the number of wells, and time at one's disposal, using this strategy might be able to quickly improve the well-by-well match but is likely to hit resistance to further change just as quick. The more wells and the more nonlinear a displacement is, the more unlikely a strategy of this sort will prove successful. A simple "conflict" map is shown in Figure 15. The red cells represent cells where conflicting values of c^* have been mapped down to the same location. In other words, a red cell is a cell where at one time a value of $c^* > 1$ may have been found and at a later time a value of $c^* < 1$. Conflicts arise because information from more than one time step is being averaged together. An extreme conflict map might be an

indication that the original model is not a good starting point and/or that the all wells all timestep strategy might not be the best strategy to deploy.

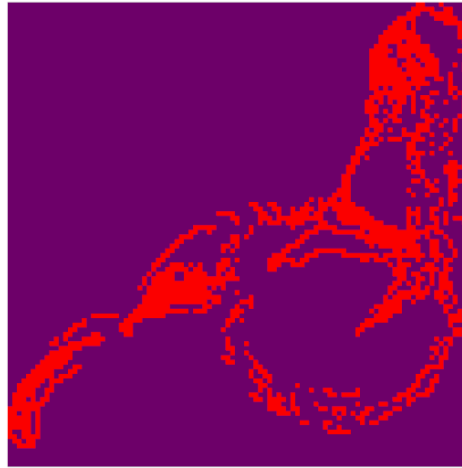


Figure 15: Conflict map for a simple 2D case. Red cells are cells where both $c^*>1$ and $c^*<1$ have been mapped to in an all wells all timestep strategy.

Final thoughts on HM strategies

There is no optimal strategy, and the four strategies outline above represent the limiting cases of in-between strategies. A successful approach of the SLAHM methodology might require starting out with one strategy and then moving over to another. Available time and computer resources are also a factor in choosing the strategy. Ultimately however, proper selection of strategies is likely to become apparent during the HM process itself and will be up to the reservoir engineer to recognize what works and what doesn't. No amount of sophisticated software will be able to remove the participation of the engineer in strategy selection and this is one reason why history matching is likely to remain an "assisted" workflow for some time.

EXAMPLE: JUDY CREEK 'A' POOL WATERFLOOD/HCMF

The Judy Creek Beaver Hill Lake 'A' oil pool is located 200 km (124 miles) northwest of Edmonton, Alberta, Canada, and was discovered in 1959. A waterflood started in 1962, followed by a hydrocarbon miscible flood (HCMF) in 1985. Due to the ongoing development of this field, a new integrated reservoir study was undertaken to aid in future development planning. A key finding of the geologic portion of the study was a significant revision upwards to the pool STOOIP.

Judy Creek is an ideal candidate for SL flow-modeling because of the large field size, long historical production period, and effective pressure maintenance operation. The application of SL simulation to the Judy Creek Pool has been presented by *Batycky et al (2007)*.

Geological Model Description

Geologically, the Judy Creek reservoir is an atoll-like limestone reef complex of late Devonian age. The complex reaches a maximum thickness of ~ 67 m (220 ft), and covers approximately 122 km² (47 sq. miles). The reef has a highly porous organic margin, which surrounds a more stratified interior lagoon. The reef margin exhibits excellent porosity, vertical and horizontal permeability, with the best reservoir preserved on the high energy northeast margin. The lagoon is generally characterized by lower porosity and permeability, and poorer horizontal and vertical reservoir continuity.

Core studies have defined five cycles of reef growth (R-1 to R-5) (Figure 16). These cycles became progressively smaller until the reef was drowned and encapsulated by deep water shale and lime-mudstones of the Waterways Formation. The reef stages generally consist of a variety of facies, varying from shallow water lagoon and reef margin to deeper water foreslope sediments. The structurally highest point of the reservoir is located along the northeastern edge, from which the reef dips towards the southwest at approximately 8 m/km (42 ft/mile).

As part of the integrated reservoir study, a new 3-D full-field geologic model was developed following a workflow that involved building a stratigraphic framework, creating a model grid, depositional facies analysis, facies modeling, porosity and permeability modeling and upscaling. Geostatistical techniques were employed to help define the range of uncertainties for volumetric evaluation. A P50 (in terms of STOOIP) geologic model, that represents the median of 70 realizations, was used for reservoir flow simulation.

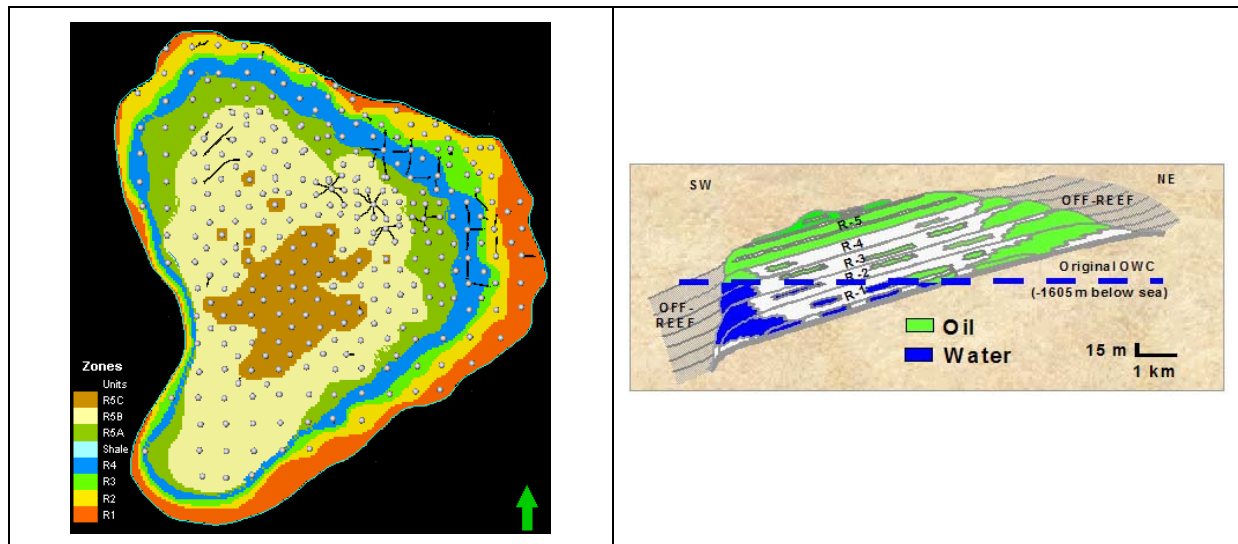


Figure 16: Judy Creek 'A' Pool Zonal Units (left) and cross section of the reef complex (right).

Production/Injection History

Oil was first produced from Judy Creek 'A' pool in December 1961. To maintain reservoir pressure, peripheral water injection was initiated at the southwest corner of the reservoir in 1962. In 1974, pattern waterflooding commenced in the northeast reef margin and interior lagoon, using existing and new wells to form inverted 5-spot patterns.

A pattern hydrocarbon miscible flood, using an ethane-based solvent, was implemented in 1985 to counter the oil decline. A summary of field historical production is shown in Figure 17. Chase gas was injected after the target solvent bank size of 15% to 20% hydrocarbon pore volume [HCPV]) was achieved. In 1997, for economic reasons it was decided that future miscible flood patterns would only inject solvent, without any chase gas to follow.

To increase volumetric sweep by solvent injection, a horizontal well injection pilot was successfully implemented in 1996. Subsequently, more horizontal miscible flood injectors were drilled to improve sweep efficiency and incremental oil recovery. These horizontal injectors were generally placed in the better quality shoal and reef margin regions in the northeast quadrant of the

pool. The new HCMF and waterflood patterns as well as strategically placed infill producers resulted to sustain oil production rates at a relatively stable level since 1998.

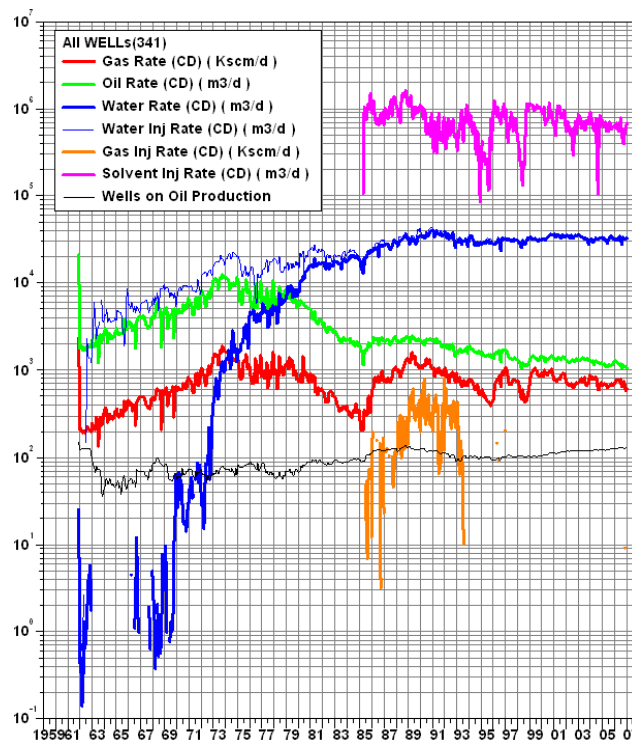


Figure 17: Judy Creek 'A' Pool Production/Injection History

Flow Simulation Model Description

The flow model has a grid of 185x211x37 (1.4 million cells), of which 600,000+ cells are active. The average cell size is 70 m x 70 m x 2 m (230 ft x 230 ft x 6.6 ft). The overall workflow of the history match process was a top-down approach like that described by Baker (2001, 2002): first a field-level match was pursued by adjusting global parameters like relative permeabilities and PVT properties, which was then followed by an individual well-level match by adjusted the local petrophysical properties. These two levels are described next.

Field-Level History Match

Sensitivity runs were made over the entire historical period to adjust global parameters such as PVT properties (oil viscosity, solution GOR), relative permeabilities (saturation end-points and curvature), miscible flood mixing parameters, oil-water contact [OWC] depths, and perforation depths to obtain a field-level history match. To reduce runtimes, production history was lumped into 1-year intervals, after determining that there were insignificant differences for both well and field level simulation results between yearly and semi-annual lumping of well events during the water flooding period. Annual lumping was also used for the miscible flood period, but we did see some sensitivity in the final results when forcing smaller timestep sizes. This was assumed to be a result of the more non-linear nature of miscible as opposed to water flooding, the former being more sensitive to timestep size. Thus, implicit in the history match is a timestep size, suggesting that forecasting should use similar annual timestep sizes to be consistent.

As shown in Figure 18, an excellent history match for oil and water was obtained at the field level. Although not shown, a similar quality match exists for the solvent production. A 46-year HM run

required approximately 10.5 hours CPU time on a Pentium IV-3.4Ghz extreme processor with 2GB of RAM.

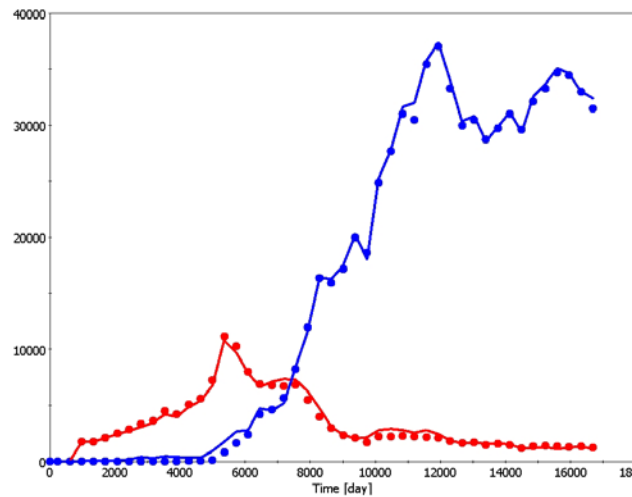


Figure 18: Initial field level match. Red is oil rate, blue is water production rate, bullets are historical data, and solid lines are simulated results.

For a 300⁺ well field there are many ways to assess the history match on a well-by-well basis. One summary of the match is based on cumulative oil production simulated versus historical to the end of 2006 for each producer (Figure 19). Clearly there is a spread in the mismatch with some wells over-producing and other wells under-producing. This figure also shows the wide range in absolute produced volumes, with the majority of producers having cumulative production of less than $2.0 \times 10^5 \text{ m}^3$ (1.26 MMbbl).

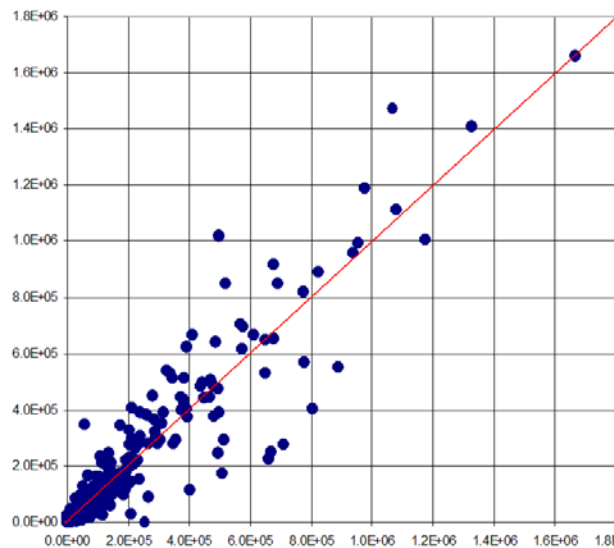


Figure 19: Simulated vs historical cumulative oil production to 2006 for each producer for the field-level history matched model (initial model).

Well-Level History Matching Workflow

Improving the history match at the well-level requires adjusting local geologic parameters. The difficulty with all well-by-well matches, but in particular for large models such as Judy Creek, is how to easily identify where these changes need to be made. In applying the SLAHM approach to

Judy Creek, we face three key elements: (a) how to update and manipulate the geology around the wells after a single flow simulation give the 1.4 million cells; (b) the selection of timesteps to history match on; and (c) the selection of wells to history match on. Both the timestep and well selection are essentially driven by engineering judgment, which further underlines the “assisted” nature of SL-based history matching.

Geology Updating

To summarize, SLAHM centers on computing grid block multipliers (c^* 's) on a per-well, per-timestep basis from the mismatch between simulated and historical water production profiles. The c^* represents the desired time-shift: values greater than 1.0 mean that faster breakthrough (shorter time-of-flight) is required, while values less than 1.0 imply that slower breakthrough (longer time-of-flight) is required. The spatial location of the SL's are used to determine which gridblocks the multipliers belong to. These c^* 's are then used to modify the input data in the generation of a new geomodel. The flow simulation is repeated, history matching errors recomputed along with the c^* 's, the geomodel rebuilt, and the process repeated until an acceptable history match is achieved. Because the c^* corrections are not mapped directly to the grid, but instead are used to update the prior model, the permeability field remains geologically realistic in an effort to force a history match. This is particularly important if the initial realization is a poor guess (a poor match) to the required geology.

In this application, we propose skipping the geological consistency step. This means that there is no need to parameterize the geology from the initial model², since there is no need to re-build a geological model after computing c^* 's. Instead, the multipliers are applied directly to permeability on the grid resulting in the workflow shown in Figure 20. Although the lack of geological consistency is drawback, it is in part off-set by not needing to re-characterize the geology; expecting a faster convergence of the well-by-well matches due to the direct changes on the grid, and not expecting too dramatic changes assuming the geological model is reasonable to begin with.

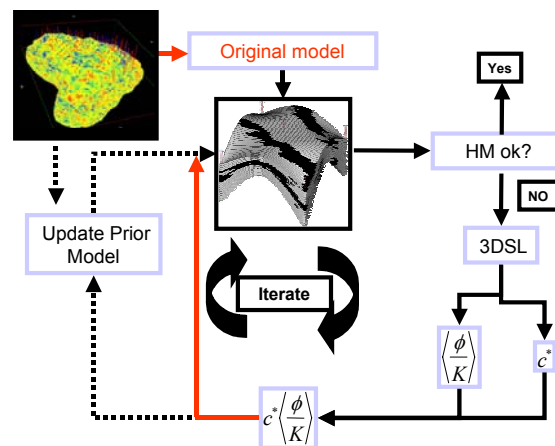


Figure 20: Schematic of how the geological model is updated after a flow simulation. The dashed arrows show the original workflow while the red arrows indicate the short cut we take when skipping the requirement of geological consistency.

² Most simulation models that require history matching are generally passed to the reservoir engineer with little or no information as to how the geostat model was produced in the first place. For the SLAHM approach where geological consistency is a key component, this means that somehow the current petrophysical distribution has to be used to extract a parametric model of the geostatistics. By skipping the geo-consistency step as in this application, has the direct advantage that there is no need to extract a geostatistical model from the original perm/poro distribution.

The mapping of the multipliers directly to the current geological model, is essentially the approach proposed by Wang and Kovscek (2000). We term this “smart-painting”, as the method is similar to using the box-type multipliers that reservoir engineers have routinely employed in manual history matches, but now the box shapes are based on the streamline bundles. Using this approach, however, will result in locally inconsistent geological characteristics (see Figure 10). We return to this point later.

Timestep Selection and Model Updating

Within each geology update loop in Figure 20, between the *SL* runs and the c^* computation, a decision needs to be made as to which time steps to use. Recall that the c^* 's reflect the mismatch for a particular well at a particular time step. One can choose to use mismatches at early times, late times, or a combination of all time steps, to compute the c^* 's and then update the model. For Judy Creek, a sequential time step selection process was used, starting with early timesteps and progressively moving to later time steps. A sequential approach is justified by the assumption that corrections for early time steps should also improve matches at later time steps, and thus as the history match progresses to later times, less corrections are needed in the model. The sequential time step process is illustrated in Figure 21.

One detail of the sequential process is the selection of timesteps for c^* computation. After a model update, the flow simulation using the update model is performed from time, $t_0=0$, to some future time t_n . For each model update we lumped c^* 's from the t_{n-2} and t_{n-3} times steps to compute average c^* . The model was updated and a flow simulation to the same time step (t_n) repeated and c^* computed, until the match was acceptable. We then moved to the next 2 timestep periods. The final two timesteps in a simulation were used as a view into the future of how each well was performing based on corrections at the earlier timesteps. If the match was deemed OK for all the wells over the t_{n-1} and t_{n-0} timesteps, then these final two timesteps became the new timesteps to compute c^* 's from and the next simulation was run to a new end time.

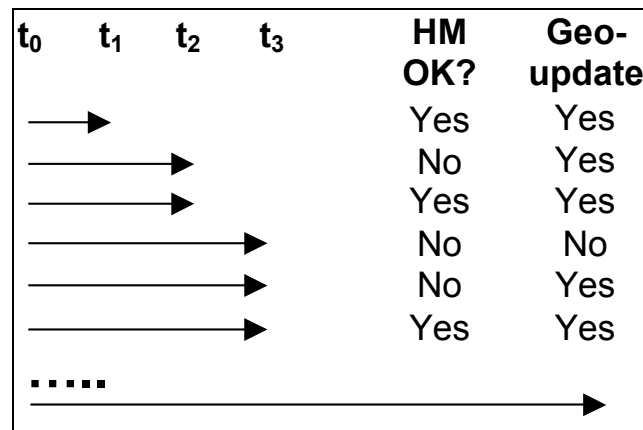


Figure 21: Sequential timestep process for history matching and updating of the geological model.

Lacking the check for geological consistency, the c^* 's were limited to a range between 0.75 and 1.25. Limiting the c^* became necessary as wells that had a large mismatch would have very high or low c^* 's, yet we wanted to ensure a gradual change of the grid properties. Allowing a wide range in c^* 's could also cause wells that were originally matching to be off again, particularly for time steps where more and more wells were used in the matching process. Finally, absolute permeability limits between 0.1 mD & 10 D for X/Y, and 0.1 mD to 5D for Z were set.

Well Selection.

Once specific timesteps were selected for history matching, a further selection was made for which wells to use for c^* calculations. Blindly selecting all wells active in a desired timestep can lead to conflicting c^* 's. In other words, inevitably some gridblocks require a permeability increases to improve the match of a given well, whereas for a different well the same gridblocks will require a permeability decreases. By using a well selection, more weighting can be given to higher rate wells.

As a first pass criterion, all active wells that had a water rate mismatch of less than 10 m³/d between simulation & historical water volumes were ignored. However, given the large variability in well liquid rates for Judy Creek, additional producers were ignored if their % water rate mismatch was less than 10%. Engineering judgment was also used to add back wells that could benefit from (small) corrections at early times in order to reduce a large mismatches at later timesteps. In other words, where possible an attempt was made to correct problems at earlier timesteps before arriving at a timestep where a large error and thus a large correction would be required.

There were some model updates that were rejected because of a degradation of the history match for some wells. Typically the correction factor for the problem well was either rejected or reduced, the geomodel recomputed from the remaining c^* 's and the previous geomodel, and the run repeated.

History Matching Results

The history matching workflow was started with timestep 6 (2072 days), 3 years after the start of water injection, and proceeded in a sequential manner until timestep 17 (6089 days). This required approximately 31 model updates over the 11 years of waterflood history. There were also about 5 updates that were rejected due to a worsening of the history match for specific wells. For these cases, adjustments were made to the c^* 's & well filters, the model was re-updated from the previous best update and the sequential process continued.

Due to project time constraints, the entire waterflood period prior to gas injection was not matched. Interim results continued to show a mismatch for some large rate producers during the gas injection period. Thus the history match workflow skipped ahead to those timesteps (9377-10107 days) and focused on improving the match for specific additional producers. Eleven more model updates were included over this period. We observed for these later times with more producers present, gridblock multipliers could adversely affect wells already reasonably matched.

Comparison of Static Models.

In total, 42 permeability updates were made starting from the original geological model. Shown in Figure 22 are the x-permeability distribution for the initial and final 3-D geological models. Recall that the final model was constructed by successively applying streamline-based multipliers to each intermediate model, rather than always applying the latest multipliers to the original model. Thus there are areas where permeabilities were successively multiplied up or down many times as can be seen by the greater highs (red) and lows (blue) in the final model.

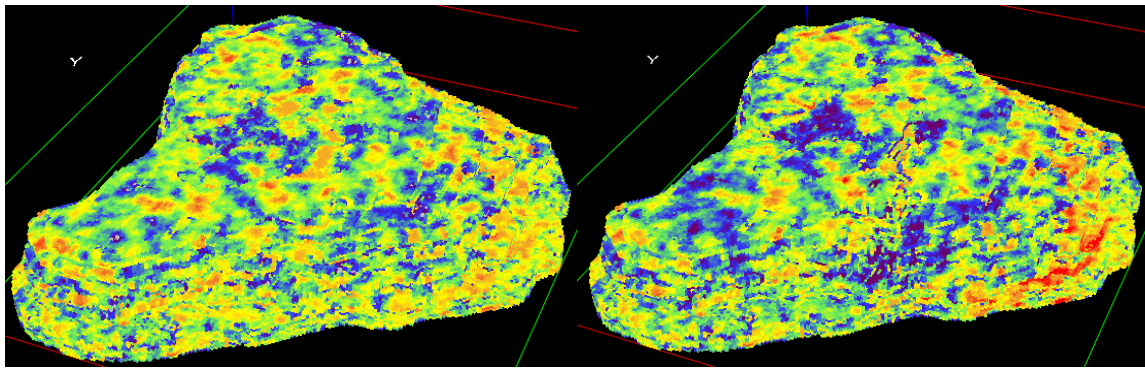


Figure 22: X-Permeability distribution for initial model (left) and X-Permeability distribution for final model (right). Color scale is log-based ranging from 0.1 to 10000 (blue to red).

Figure 22 also shows that overall geological features were well preserved, despite some minor “streamline-like” patterns appearing. Although not shown here, a comparison between the two permeability fields on a layer-by-layer basis gives similar results, with overall trends preserved, but some local streamline-like features.

Correction Factors Mapped to Grid.

To understand why the final permeability model is not dominated by streamline-like features as one might expect, consider how the successive update of multipliers were applied. The workflow started from a realistic geological image. Because the c^* 's are multipliers to permeability (limited to $0.75 < c^* < 1.25$) small values tend to remain small while large values in permeability tend to remain large. Next, correction factors were applied sequentially. Shown in Figure 23 are the gridblock multipliers based on updates 30, 31, and 32 using time intervals at 5724 days, 6029 days and 6029 days again. For illustrative purposes we've considered only layer 28 as this layer had substantial changes throughout, but similar conclusions could be drawn for other layers.

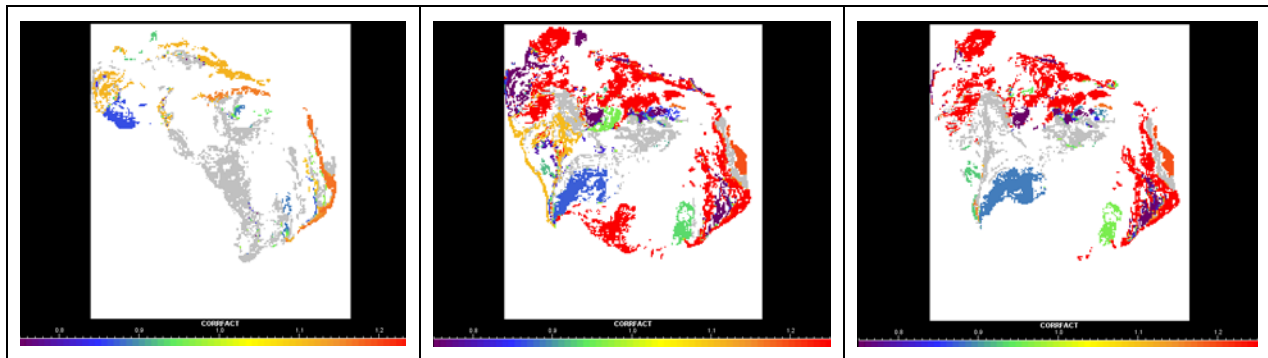


Figure 23: c^* multipliers for simulation layer 28 at: 5724 days from run 30 (left), 6029 days from run 31 (middle), and 6029 days from run 32 (right)

Note that there are significant differences in the value and location of the multipliers as a function of the timestep. In other words, changing historical well rates leads to changing streamlines, changing mismatches, and thus changing location of the resulting c^* map. Second, note that repeated corrections from successive simulations of the same timestep do not result in the same streamline locations or values of the correction factor (Figure 23 middle compared to right), and finally as the match improves for a particular timestep, future updates for the same timestep require less correction. As a result, the process of applying successive correction factor maps tends to destroy previous trends that can be associated with streamline locations.

Comparison of Field Level Production Results.

As shown in a previous section, the field level match prior to history matching was already quite good. Here we again show the field level match to ensure that well-level matching did not make the overall match worse. This is possible since not all the wells were included in the history match.

Figure 24 shows a comparison of the field oil rate match before and after the history matching process. Although the match was good to begin with—due to changes in global parameters—it improved further, particularly over the time period between about 6000-8000 days. There is also some improvement after gas injection start up (9377 days) although the history matching process was only cut-off at 10107 days. The field water rate match is quite good for both initial and final models (Figure 25).

Figure 24 also shows the oil rate field match for the final permeability model but with the PVT properties (miscible mixing parameters) of the initial model. What the comparison between this model and the initial and final models shows is how the miscible parameters of the initial model needed to be recalibrated once the geology was modified, so as to again match field-level oil production (dashed red line), particularly for the final timesteps. Recall that the miscible parameters were tuned to give a good overall field match for the miscible portion. Implicit in the original values were such factors as timestep size, grid resolution, and most importantly geology. As a result of geology changes, the mixing parameters were again tuned to new values to give a good match of field level oil rate for the final timesteps. This inability to completely decouple fluid physics from the simulation grid is well known and originally noted by Todd and Longstaff (1972), where they observed a dependency between the value of their mixing parameter and the description of the porous medium, both of which determined the size of the miscible zone.

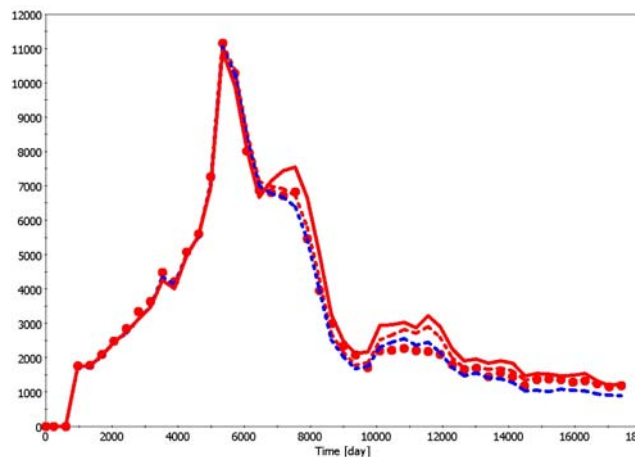


Figure 24: Field oil rate comparison between the initial model (solid line), final model (dashed line) and historical data (bullets). The blue-dashed line is the final model permeability field, but with the relative permeabilities and PVT of the initial model.

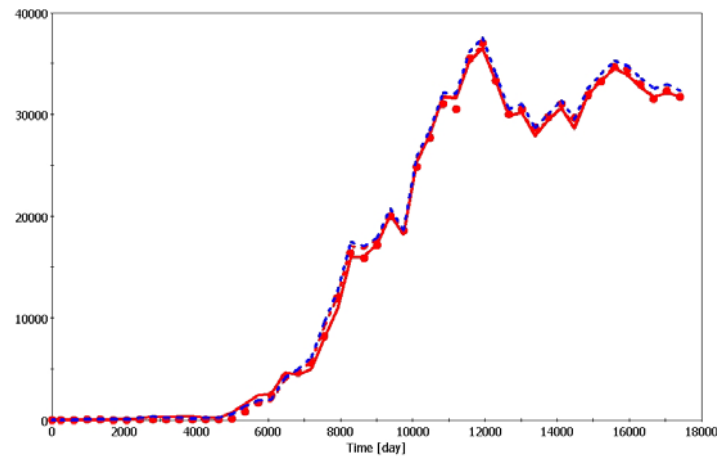


Figure 25: Field water rate comparison between the initial model (solid line), final model (dashed line) and historical data (bullets). The blue-dashed line is the final model permeability field, but with the relative permeabilities and PVT of the initial.

Comparison of Well Level Production Results

As a single metric to summarize the well-level match, we again show a cross-plot of simulated vs historical cumulative oil production for the final run (Figure 26-left). When compared to the original well-by-well mismatch (Figure 26-right), it is clear that the final model is an improvement even on a well-by-well basis. Wells used in the history match appear colored in purple Figure 26. As one might expect, wells that were not included in the history matched also showed improvement.

The cross-plots in Figure 26 are not sensitive to producers that over produced and then under produced but have the correct cumulative volume on average. They also do not highlight changes between runs in a single graph. Thus, an additional metric to compare pre- and post-matched runs is through each well's objective function (OF). Here we use the L2-Norm of the water production rate—the square-root of the sum of the squared difference in water rates. The L2-norm however, does not discriminate between low and high rate wells. Large rate wells with the same delta rate mismatch as small rate wells appear as equals.

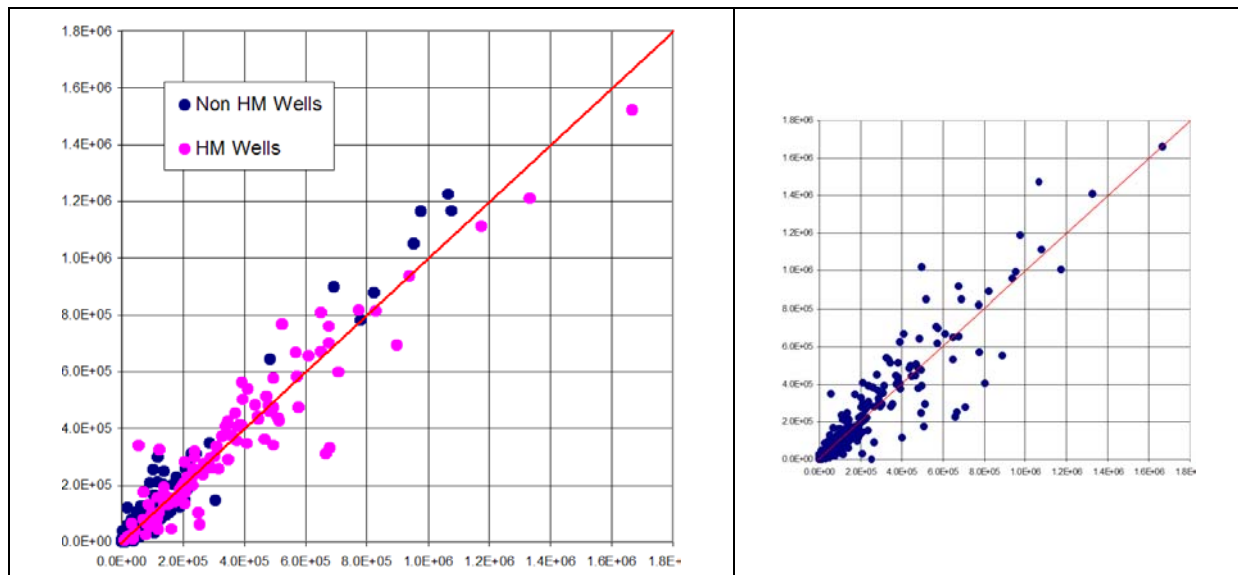


Figure 26: Simulated vs historical cumulative oil production to 2006 for each producer for the final well-level history matched model (final model). Pink bullets are the wells included in the history matching while blue bullets are the remaining producers. Correlation coefficient for all the above data is 0.966.

Shown in Figure 27 is a cross-plot of the final L2-norm and the initial L2-norm of each well. In this case, an improvement of the match occurs if more points fall below the diagonal than above the diagonal. The purple points represent producers that were history matched, while the blue points are for the remaining producers. The majority of the purple points are clearly below the diagonal.



Figure 27: Objective function of each producer for the final well-level history matched model vs the initial model.

Both the cumulative comparison and the objective function comparison show that some well matches were made worse after history matching. This is a well known fact and does not need to be elaborated on except to say that not all wells were included in the history matching workflows nor were all timesteps. The model was matched up to about 10107 days, yet the complete simulation covers up to 17142 days. Furthermore, even in a fine model with 600,000⁺ cells will lack geology trends that are truly present and there might still be is not enough detail in the flow model, even between many infill producer/injector pair.

Some example well-level history match comparisons are shown in Figure 28. These wells were selected based on various outlier points in the cumulative cross-plot and the objective function cross-plot.

The highest cumulative oil producer shown on Figure 26, 0409NE, is also a well with the greatest increase in its OF (6.8 to 27.1). The water production for 0409NE is shown in Figure 28. Although this well did show a large increase in its OF, the overall match is still quite good. In fact, the large OF value is misleading and is more a reflection of the large absolute water rates for this well.

Another producer with a large increase in its OF (3.7 to 9.3) is 0425SW, as there is substantial water production. A primary reason for the poor final match is that a nearby producer, 0225SW, required changes to permeability to promote earlier water production. This might be an example where despite the fine resolution of the overall model, the local resolution between wells might still be too coarse.

A producer with a large decrease in objective function is 1201NW (OF 13.8 to 1.6). As shown in Figure 28, high early water production has been substantially reduced. History matching was only done up to about 10000 days for this well.

A large historical cumulative oil volume ($7.07 \times 10^5 \text{ m}^3$, 4.45 MMbbl) producer is 0203NW which had a decrease in its OF from 18.5 to 4.5. Water and oil production are shown in Figure 28 with its greatest mismatch and improvement early on between 4000-7000 days. After 7000 days, there appears to be little difference in water production between the initial and final models. However, because of the 90%+ watercut after 700 days, it is also instructive to look at this well's oil rate comparison separately. As can be seen, the oil production plot reveals a doubling in oil rate after 7000 days. Even though corrections were applied to this well within the first 4000-7000 days, this is a good example of how early corrections improve the match at much later time periods.

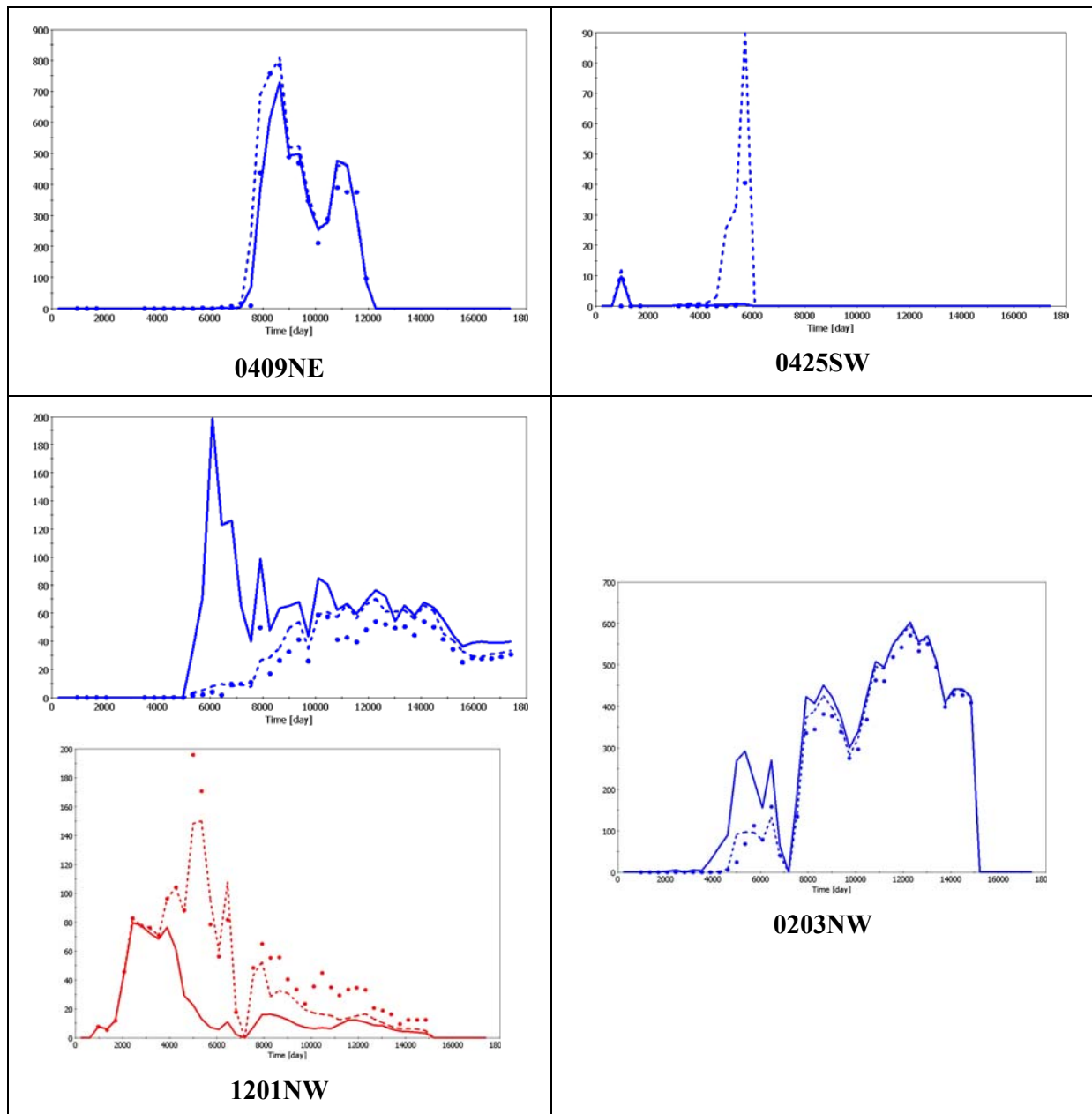


Figure 28: Some example well-level history matches. Bullets are history, solid line is initial model, and dashed line is the final model. From top-left going clock-wise: water production rate for Well 0409NE; water rate for well 0425SW; water rate for well 0203NW ; water and oil production rate for well 1201NW

Impact on Solvent Injection Period

Only the difference between simulated and historical water production was used to decide where to make corrections and the magnitude of corrections to apply. Additionally, only the waterflood signature to about 10107 days was used. Gas injection started at about 9377 days to 17142 days. So not only were produced solvent signatures ignored, but there was also a significant portion of the solvent injection time period whose waterflood signatures were unmatched. Yet it was still observed that well-level matches over the solvent period improved (for example 0203NW).

Conclusions for the Judy Creek Study

1. “Smart-painting” can be an effective means to improve well-level history matches when geological modeling capabilities are missing or turn-around times are to be reduced. This is particularly true when starting with a reasonable geomodel or if the multipliers required to achieve a history match are reasonable. In the Judy Creek case, smart-painting did not result in an unrealistic final geological model.
2. Gridblock resolution and production history resolution affect the resolution of the c*’s maps that are painted to the grid, which in turn limits the accuracy of the final history match.
3. The workflow presented here allows for automatic updating of the gridblock properties, something needed for large geological models. However, there is still a strong “assisted HM” component for well selection and timestep selection.
4. Although not all timesteps or wells were included in the well-level history match, improvements were also seen for wells excluded from the history match. Similarly, although only water mismatch signatures were used to update the geology, improvements in field level oil production during gas injection were also observed.
5. Because of the complexity of fluid displacements and the difficulty in completely decoupling geology from flow physics, we observed that field wide PVT parameters for the miscible model needed to be re-tuned at the field scale once geology changes at the well-level were completed. This was expected since these global parameters are an implicit function of the geology, grid resolution, and timestep size.

ACKNOWLEDGMENTS

We would like to thank Lisette Quettier, Bernard Corre, Peter Behrenbruch, John Gardner, and Tom Schulte for their foresight and early recognition of the potential of SL simulation, and their support for the industrial development of the technology.

We would like to thank members of the Streamsim/Stanford Streamline-Based Assisted History Matching Joint Industry Project for their support.

The authors wish to acknowledge Pengrowth management’s permission to publish results of the Judy Creek example and the support of Pengrowth’s geoscience team.

REFERENCES

1. 3DSL, User Manual v2.30, Feb 2007, Streamsim Technologies.
2. Agarwal, B. and Blunt, M.J.: "A Full-Physics, Streamline-Based Method for History Matching Performance Data of a North Sea Field," paper SPE 66388 in proceedings of the Reservoir Simulation Symposium, Houston, TX (February 2001).
3. Agarwal, B. and Blunt, M.J.: "A Streamline-Based Method for Assisted History Matching Applied to an Arabian Gulf Field," *SPE Journal* (December 2004) 437-449.
4. Batycky, R.P.: "A Three-Dimensional Two-Phase Field Scale Streamline Simulator," PhD Thesis, Stanford University, Dept. of Petroleum Engineering, Stanford, CA, 1997.
5. Batycky, R.P., Thiele, M.R., Baker, R.O. and Chug, S.H.: "Revisiting Reservoir Flood Surveillance Methods Using Streamlines," *SPE Reservoir Engineering* (xxx 2007) xxx-xxx.
6. Batycky, R.P., Blunt, M.J., and Thiele, M.R.: "A 3D Field Scale Streamline-Based Reservoir Simulator," *SPE Reservoir Engineering* (November 1997) 246-254.
7. Batycky, R.P., Seto, A.C., and Fenwick, D.H.: "Assisted History Matching of a 1.4-Million-Cell Simulation Model for Judy Creek 'A' Pool Waterflood/HCMF Using a Streamline-Based Workflow," proceedings of the SPE ATCE, Anaheim, CA, 11-14 November (2007).
8. Baker, R.A.: "Streamline Technology: Reservoir History Matching and Forecasting – Its Successs, Limitations, and Future," Distinguished Author Series, JCPT, April 2001, Vol 40, No. 4, pp. 23-27.
9. Baker, R., Kuppe, F., Chug, S., Bora, R., Stojanovic, S., and Batycky, R.P.: "Full-Field Modeling Using Streamline-Based Simulation: 4 Case Studies" *SPEE* (2002) **5**(2), 126-134.
10. Bommer, M.P. and Schechter, R.S.: "Mathematical Modeling of In-Situ Uranium Leaching," *SPEJ* (December 1979) 19, 393-400.
11. Bratvedt, F., Gimse, T. and Tegnander, C.: "Streamline computations for porous media flow including gravity." *Transport in Porous Media*, Vol. 25, No. 1, 63-78 (Oct. 1996).
12. Bratvedt, F., Bratvedt, K., Buchholz, C., Holden, L., Holden, H., and N.H. Risebro: "A New Front-Tracking Method for Reservoir Simulator," *SPE Reservoir Engineering* (February 1992) 107-116. Caers, J. "Petroleum Geostatistics", SPE Primer Series, 2005. Caers, J. "Efficient Gradual Deformation Using a Streamline-Based Proxy Method" *Journal of Petroleum Science and Engineering*, **39**, 2003, 57-83. Caers, J., Krishnan, S., Wang, Y. & Kovscek, A. R.: "A Geostatistical Approach to Streamline-based History Matching" *SPE Journal*. **7**(3) September 2002, 250-266.
16. Carlson, M.R., "Practical Reservoir Simulation: Using, Assessing, and Developing Results," PennWell Books, 2003.
17. Cheng, H., Osako, I., Datta-Gupta, A., and King, M.J.: "A Rigorous Compressible Streamline Formulation for Two- and Three-Phase Black-Oil Simulation," paper SPE 96866 in proceedings of the 2005 SPE ATCE, Dallas, TX (9-12 Oct).
18. Datta-Gupta, A. and King, M.J.: "A Semi-Analytic Approach to Tracer Flow Modeling in Heterogeneous Permeable Media," *Advances in Water Resources* (1995) **18**(1), 9-24.
19. Di Donato, G., Huang, W., and Blunt, M.J.: "Streamline-Based Dual Porosity Simulation of Fractured Reservoirs," SPE 84036 proceedings of the SPE Annual Technical Conference and Exhibition Denver, Colorado, U.S.A., 5 - 8 October 2003.

20. Di Donato, G. and Blunt, M.J.: "Streamline-based dual-porosity simulation of reactive transport and flow in fractured reservoirs," *Water Resources Research*, **40**, W04203, doi:10.1029/2003WR002772 (2004).
21. Emanuel, A.S. and Milliken, W.J.: "Application of Streamtube Techniques to Full-Field Waterflooding Simulation," *SPERE* (August 1997), 211-217.
22. Emanuel, A.S. and Milliken, W.J.: "Application of 3D Streamline Simulation to Assist History Matching," SPE paper 49000 in proceedings of the 1998 ATCE, New Orleans, LA (October).
23. Fenwick, D.H., Thiele, M.R., Agil, M., Hussain, A., Humam, F., and Caers, J.: "Reconciling Prior Geologic Information with Production Data Using Streamlines: Application to a Giant Middle-Eastern Oil Field," SPE paper 95940 in proceedings of the 2005 ATCE, Dallas, TX (9-12 October).
24. Glimm, J. *et al*, "Front Tracking Reservoir Simulator, Five-Spot Validation Studies and the Water Coning Problem," *The Mathematics of Reservoir Simulation*, R. Ewing (Ed.), SIAM, Philadelphia (1983) 107-36.
25. Hoffman, B.T., and Caers, J.: "Regional probability perturbations for history matching," *Journal of Petroleum Science and Engineering*, 2005 **46**: 53-71.
26. Ingebrigtsen, L., Bratvedt, F. and Berge, J.: "A Streamline Based Approach to Solution of Three-Phase Flow", SPE 51904 in proceedings of the SPE Reservoir Simulation Symposium, Houston, TX, 14-17 February 1999.
27. King, M.J., Blunt, M.J., Mansfield, M., and Christie, M.A.: "Rapid Evaluation of the Impact of Heterogeneity on Miscible Gas Injection," paper SPE26079 in proceedings of the Western Regional Meeting, Anchorage, AK (1993).
28. Le Ravalec-Dupin, M. and Fenwick, D.H.: "A Combined Geostatistical and Streamline-Based History Matching Procedure," paper SPE77378 in proceedings of the 2002 ATCE, San Antonio, TX, 29 Sept.–2 Oct. 2002.
29. Mattax, C.C., and R.L. Dalton, "Reservoir Simulation," SPE Monograph, Vol 13, Henry L. Doherty Series, 1990.
30. Martin, J.C. and Wegner, R.E.: "Numerical Solution of Multiphase, Two-Dimensional Incompressible Flow Using Streamtube Relationships" *Society of Petroleum Engineers Journal* (October 1979) 19, 313-323.
31. Muskat, M. and Wyckoff, R.: "Theoretical Analysis of Waterflooding Networks," *Trans. AIME* (1934) 107, 62-77.
32. Pollock, D.W.: "Semianalytical Computation of Path Lines for Finite-Difference Models," *Ground Water*, (November-December 1988) 26(6), 743-750.
33. Renard, G.: "A 2D Reservoir Streamtube EOR Model with Periodic Automatic Regeneration of Streamlines," *In Situ* (1990) **14**, No. 2, 175-200.
34. Samier, P., Quettier, L., and Thiele, M.: "Applications of Streamline Simulations to Reservoir Studies," *SPERE* (2002) **5**(4), 324-332.
35. Stüben, K.: Algebraic Multigrid (AMG): An Introduction with Applications. Guest appendix in the book "Multigrid" by U. Trottenberg; C.W. Oosterlee; A. Schüller. Academic Press, 2000.
36. Thiele, M.R., Blunt, M.J., and Orr, F.M.: "Modeling Flow in Heterogenous Media Using Streamtubes—II. Compositional Displacements," *InSitu* (November 1995) 19, No. 4, 367.

37. Thiele, M.R., Batycky, R.P., Blunt, M.J., and Orr, F.M.: "Simulating Flow in Heterogeneous Media Using Streamtubes and Streamlines," *SPE Reservoir Engineering* (February 1996) 10, No. 1, 5-12.
38. Thiele, M.R., Batycky, R.P., and Blunt, M.J.: "A Streamline Based 3D Field-Scale Compositional Reservoir Simulator," SPE paper #38889 in proceedings of the 1997 ATCE, San Antonio, TX (October).
39. Thiele, M.R. and Batycky, R.P.: "Discussion of SPE65604—Streamline Simulation: A Technology Update," *Journal of Petroleum Technology* (May 2001), **53**, No.5, 26-27
40. Thiele, M.R., Batycky R.P., and Kent, L.T.: "Miscible WAG Simulations Using Streamlines," in proceedings of the 8th European Conference on the Mathematics of Oil Recovery (ECMOR), Freiberg, Germany, 3-6 Sept., 2002.
41. Thiele, M.R. and Batycky, R.P.: "Water Injection Optimization of a Giant Carbonate Field Using a Streamline-Based Workflow," SPE 84080 in proceedings of the SPE ATCE, Denver, CO, 5-8 October 2003.
42. Todd, M.R. and Longstaff, W.J.: "The Development, Testing, and Application of a Numerical Simulator for Predicting Miscible Flood Performance," *Journal of Petroleum Technology* (July 1972) 874-882.
43. Vasco, D.W., Yoon, S., and Datta-Gupta, A.: "Integrating Dynamic Data into High-Resolution Reservoir Models Using Streamline-Based Analytical Sensitivity Coefficients," *SPE Journal* (4) 389-399 (1999).
44. Wang, Y. and Kovscek, A.R.: "Streamline Approach for History Matching Production Data," *SPE Journal* (4), 353-362, (December 2000).
45. Wen X.-H., Deutsch, C.V., and Cullick, A.S.: "A Fast Streamline-Based Method for Computing Sensitivity Coefficients for Fractional Flow Rate," SPE paper 50693 in proceedings of the 1998 ATCE, New Orleans, LA (October).
46. Wu, Z. and Datta-Gupta, A.: "Rapid History Matching Using a Generalized Travel-Time Inversion Method" *SPE Journal* Issue Vol 7, Number 2, June 2002 Pages 113-122
47. Williams, G.J.J., Mansfield, M., MacDonald, G., and Bush, M.D.: "Top-Down Reservoir Modeling," SPE paper 89974 in proceedings of the 2004 ATCE, Houston, TX (26-29 Sept.).